

6575  
2-R-P.

BRITTLE FRACTURE

by

THOMAS PHILLIPS MELOY

A.B. Harvard University (1949)

B.S. Massachusetts Institute of Technology (1951)

SUBMITTED IN PARTIAL FULFILLMENT

OF THE REQUIREMENTS FOR THE

DEGREE OF DOCTOR OF PHILOSOPHY

October 1960

Signature of Author  
Department of Metallurgy  
October 31, 1960

Signature Redacted

Signature of Professor  
in Charge of Research

Signature of Chairman of  
Department Committee on  
Graduate Students

\_\_\_\_\_  
\_\_\_\_\_  
\_\_\_\_\_

BRITTLE FRACTURE

by

Thomas Phillips Meloy

Submitted to the Department of Metallurgy  
Massachusetts Institute of Technology

on October 31, 1960

In Partial Fulfillment of the Requirements for the Degree of  
DOCTOR OF PHILOSOPHY

ABSTRACT

A mathematical model of brittle fracture was set up. From this model was derived an equation which expresses the cumulative weight of material finer than a given size as a function of size. The equation is

$$\frac{W(x)}{W_0} = 1 - \left(1 - \frac{x}{X_0}\right)^r$$

where  $W(x)$  is the weight of material finer than a given size,  $x$ ,  $W_0$  is the initial weight of material,  $X_0$  is the initial size of the particle and  $r$  is the size ratio.

With the use of a probabilistic model of grinding an integral differential equation was set up and solved. The solution expressed the size distribution of the output of commercial grinding machines as a function of time and size.

Thesis Supervisor: Professor A. M. Gaudin

Title: Richards Professor of Mineral Engineering

## ACKNOWLEDGMENT

The author wishes to acknowledge the pleasure and privilege of writing his thesis under Professor A. M. Gaudin. He also wishes to thank Professor G. P. Wadsworth and Dr. Reese Prosser for their technical consultation and encouragement, and Dr. M. C. Fuerstenau for his encouragement to pursue the subject of brittle fracture. He also wishes to acknowledge and thank his wife for the manifold assistance and guidance given throughout his graduate work.

The author is indebted to the National Science Foundation for its support while working on the thesis and the International Business Machines Company for the use of their machines at the MIT Computational Center, Cambridge, Mass., where part of this work was done.

TABLE OF CONTENTS

Introduction.....1  
Definitions.....3  
Single Fracture.....6  
Repeated Fracture.....22  
Mathematical Model of Repeated Fracture.....28  
Analytical Solutions to Equation 77.....32  
Method of Numerical Solution of Equation 77.....40  
Results.....48  
Summary and Conclusions.....78  
Suggestions for Future Work.....81  
Biographical Sketch.....83  
Bibliography.....84  
Appendix.....Vol. II

TABLE OF ILLUSTRATIONS

<u>Figure No.</u>	<u>Page No.</u>
A-1	Line Segment..... 9
A-2	Ball on Plate .....24
A-3	Ball on Curved Plate ..... 25
A-4	Ball on Ball..... 25
A-5	Stamp Mill ..... 27
A-6	Matrix..... 42
1	Comparison of the three major equations used to describe the cumulative weight finer of the fragments obtained by single fracture.....52
2	Comparison of Hukki's experimental data for galena crushed in a single-blow pendulum crusher with the equation derived in this thesis for single fracture..53
3	Experimental log-log size distribution plots of galena broken during single fracture..... 53A
4	Experimental semi-log size distribution plots of quartz ground in a rod mill for different length of time....53A
5	Experimental semi-log size distribution plots of quartz ground in a ball mill for different length of time...53A
6	Calculated plots of log percent weight retained vs. log size for different time intervals. $P(x) = 1/2$ ; $r = 2$ ..... 54
7	Calculated plots of log percent weight retained vs. log size for different time intervals. $P(x) = 1/2$ ; $r = 4$ .....55

Figure No.

Page No.

8	Calculated plots of log percent weight retained vs. log size for different time intervals. $P(x) = 1/2;$ $r = 4; s = 1$ .....	56
9	Calculated plots of log percent weight retained vs. log size for different time intervals. $P(x) = 1/2;$ $r = 8$ .....	57
10	Calculated plots of log percent weight retained vs. log size for different time intervals. $P(x) = 1/2;$ $r = 16$ .....	58
11	Calculated plots of log percent weight retained vs. log size for different time intervals. $P(x) = 1/2 x^{1/2}; r = 2$ .....	59
12	Calculated plots of log percent weight retained vs. log size for different time intervals. $P(x) = 1/2 x^{1/2}; r = 4$ .....	60
13	Calculated plots of log percent weight retained vs. log size for different time intervals. $P(x) = 1/2 x^{1/2}; r = 4; s = 1$ .....	61
14	Calculated plots of log percent weight retained vs. log size for different time intervals. $P(x) = 1/2 x^{1/2}; r = 8$ .....	62
15	Calculated plots of log percent weight retained vs. log size for different time intervals. $P(x) = 1/2 x^{1/2}; r = 16$ .....	63

16	Theoretical plots of log percent weight retained vs. log size for different time intervals. $P(x) = 1/2 x$ ; $r = 1$ .....	64
17	Calculated plots of log percent weight retained vs. log size for different time intervals. $P(x) = 1/2 x$ ; $r = 2$ .....	65
18	Calculated plots of log percent weight retained vs. log size for different time intervals. $P(x) = 1/2 x$ ; $r = 4$ .....	66
19	Calculated plots of log percent weight retained vs. log size for different time intervals. $P(x) = 1/2 x$ ; $r = 4$ ; $s = 1$ .....	67
20	Calculated plots of log percent weight retained vs. log size for different time intervals. $P(x) = 1/2 x$ ; $r = 8$ .....	68
21	Calculated plots of log percent weight retained vs. log size for different time intervals. $P(x) = 1/2 x$ ; $r = 16$ .....	69
22	Calculated plots of log percent weight retained vs. log size for different time intervals. $P(x) = 1/2 x^2$ ; $r = 2$ .....	70
23	Calculated plots of log percent weight retained vs. log size for different time intervals. $P(x) = 1/2 x^2$ ; $r = 4$ .....	71

24	Calculated plots of log percent weight retained vs. log size for different time intervals. $P(x) = 1/2 x^2$ ; $r = 8$ .....	72
25	Calculated plots of log percent weight retained vs. log size for different time intervals. $P(x) = 1/2 x^2$ ; $r = 16$ .....	73
26	Calculated plots of log percent weight retained vs. log size for different time intervals. $P(x) = \text{Comp } 1$ ; $r = 2$ .....	74
27	Calculated plots of log percent weight retained vs. log size for different time intervals. $P(x) = \text{Comp } 1$ ; $r = 4$ .....	75
28	Calculated plots of log percent weight retained vs. log size for different time intervals. $P(x) = \text{Comp } 1$ ; $r = 8$ .....	76
29	Calculated plots of log percent weight retained vs. log size for different time intervals. $P(x) = \text{Comp } 1$ ; $r = 16$ .....	77
30	Feed, 2500 grams of quartz, through 9.423 mm. and on 6.680 mm., ground for 4 hours in a batch mill with 55-7/8 inch ball weighing 3500 grams.....	77A
31	Feed, 2500 grams of quartz, through 9.423 mm. and on 6.680 mm., ground for 1 hour in a batch mill with 55-7/8 inch balls weighing 3500 grams.....	77A



Figure No.

Page No.

- 32 Feed, 2500 grams of quartz, through 9.423 mm. and on 6.680 mm., ground for 16 hours in a batch mill with 55-7/8 inch balls weighing 3500 grams.....77A
- 33 Feed, 2500 grams of quartz, through 9.423 mm. and on 6.680 mm., ground for 60 hours in a batch mill with 55-7/8 inch balls weighing 3500 grams.....77A

## INTRODUCTION

It is estimated that in the United States alone, one billion tons<sup>(1)</sup> of material are comminuted each year. Yet the efficiency of new surface produced per unit of energy consumed is far less than one percent. Thus any improvement in the comminution process would be of far reaching economic importance. However, before any real breakthrough can be expected, a greater understanding of the fundamentals of single and repeated fractures must be obtained.

Historically, the approach to understanding and predicting the output of a comminution device has been through energy. Rittinger<sup>(2)</sup> and to a lesser extent Kick<sup>(3)</sup> were the promulgators of this viewpoint. Gaudin<sup>(4,5,6)</sup> and his co-workers took another tack. They pursued the experimental approach and essentially set the guideposts to which any theoretical study must conform.

In 1941, Brown<sup>(7,8,9)</sup> and his co-workers using the Rosin-Rammler<sup>(10)</sup> empirical distribution for single fracture attempted to predict the composite distribution of the product of grinding machines. Hukki<sup>(5)</sup> did the same thing using the Gaudin-Schuhmann<sup>(6)</sup> equation. In 1948, Epstein<sup>(11)</sup> showed that the log cum weight finer vs. log size plot would be a straight line if all particles had an equal probability of being broken. The assumption that the probability of a particle being broken,  $P(x)$ , is independent of size was widely held<sup>(4,6,7,8,9)</sup>.

In 1956, Callcott and Broadstreet<sup>(12)</sup> decided to determine if and how  $P(x)$  varied with size in the grinding machines they were using. By using matrix analysis they obtained empirical values of  $P(x)$  in their

matrices. To do this, they used the same type of size distribution function that Brown<sup>(9)</sup> had used. However, they expressed the hope that a better size distribution would be derived so that they might use it in their analysis. In 1959, Gilvarry<sup>(13)</sup> derived an equation, similar to the empirical Rosin-Rammler<sup>(10)</sup> equation, both of which are of the form

$$\frac{W(x)}{W_0} = 1 - e^{-\frac{x}{b}} \quad (1)$$

$W(x)$  is the weight finer than a given size  $x$ ,  $W_0$  is the weight of the sample and  $b$  is the experimentally determined constant.

The writer has essentially done three things:

- 1) He derived a new size distribution for individual fracture.
- 2) He derived  $P(x)$  for both a ball mill and a rod mill.
- 3) He set up and solved an integral differential equation which predicts the output of grinding devices. The equation was solved both numerically and analytically.

## DEFINITIONS

Since the approach in this dissertation is new, it is necessary to define certain terms which will be used repeatedly throughout the text. The terms will be defined by referring to specific events.

Comminution event - If an ordinary drinking glass were dropped on a hard floor it would break. The breaking of the glass is a comminution event. Though many fragments are formed, they are the result of one, single, individual comminution event. If one of the fragments of the glass is later broken, then this is another comminution event.

Single Fracture - The drinking glass undergoes single fracture if it is broken during a comminution event.

Repeated Fracture - The glass would undergo repeated fracture if it were broken during a comminution event and then fragments of the glass were subsequently broken by later comminution events.

Daughter Products - When the glass undergoes single fracture the fragments are daughter products. If the daughter products are subsequently broken, they are called second generation daughter products.

Size Ratio - This is the average number of surfaces of fracture required along the characteristic dimension per original particle, to yield the product obtained. Since the daughter products vary in size, it is difficult to reconcile the size ratio with the customary reduction ratio. However, this correlation can be made whenever the feed has already been broken, viz., contains particles of all sizes. A mathematical definition is the ratio of size of the feed to size of the daughter product at the point where  $\frac{W(x)}{W_0} = 1$  in the Gaudin-Schuhmann equation.

Characteristic Shape - When a homogeneous material is broken, it breaks into a series of fragments, all of which have the same general shape. The characteristic shape varies from material to material but remains the same for a given material, irrespective of the size of the fragment.

Characteristic Dimension - If the fragments of a particle are all spheres, the characteristic dimension could be the radius or the diameter. If the fragments are rectangular prisms, the characteristic dimension could be the diagonal or one of the edges. The characteristic dimension of the fragments may be chosen arbitrarily but once chosen it must be the same characteristic dimension throughout the analysis. The cube of the characteristic dimension is proportional to the volume of the particle.

Size Frequency Distribution - When a particle, such as the drinking glass breaks, there are many fragments. The fragments are of different size, or to be more precise, the size of the characteristic di-

mension is different for each particle. If a plot is made of the frequency of occurrence of fragments of a given size versus size, there results the size frequency distribution. This is a frequency distribution of a continuous random variable and has the property of an integral between the smallest and largest sized particle which is equal to one. The size frequency distribution is a mathematical frequency distribution.

Mass Frequency Distribution - This is similar to the size frequency distribution except that the frequency of mass is plotted versus size. It, too, is a mathematical frequency distribution.

CWF or Cumulative Weight Finer - The CWF, in mathematical terms, is the cumulative frequency distribution of the mass frequency distribution. In other words, the CWF is the integral from 0 to  $x$  of the mass frequency distribution,  $x$  being any size between the smallest and largest fragment.

Gaudin-Schuhmann Equation - This is an empirical equation developed by Gaudin<sup>(4)</sup> and modified by Schuhmann<sup>(6)</sup> to express the CWF.

Weight Retained - The weight retained means the weight of fragments retained on a smaller screen while passing through the larger screen. Mathematically, it is the integral of the mass frequency distribution between a given screen size and the next larger screen size.

Half-Life - The term half life is borrowed from physics and means the time required for half of the particles of a given classification to be broken.

## SINGLE FRACTURE

This chapter is concerned with single fracture. It introduces concepts, terms and models used in discussing single fracture events. The basic assumption is that the material is homogeneous and consequently has no grain size.

A single fracture event is considered to take place instantaneously. For example, if a glass sphere is dropped on the floor and breaks this is considered as one comminution event. Many fragments may be formed but they are a result of a single comminution event or single fracture. If subsequently one of the daughter products is broken this is a second comminution event. Two comminution events cannot take place simultaneously. They must be seriated.

When a single crystal breaks, the result is many fragments. These fragments vary in size. The usual way of reporting the experimental data is to plot log weight finer than a given size versus the log size. This is called the cumulative weight finer plot. The resultant plot shows a straight line on log-log paper when the size is small compared to the largest size fragment. In the upper size ranges the empirical plot bends to the right of the straight line portion of the curves.

Three equations have been developed to describe the cumulative weight finer plot. The first is the Gaudin-Schuhmann equation:

$$\frac{W(x)}{W_0} = \left(\frac{x}{k}\right)^m \quad (2)$$

where  $W(x)$  is the weight finer than a given size  $x$ , a characteristic

dimension of the particle,  $W_0$  is the weight of the sample,  $k$  is the size modulus (or maximum theoretical size fragment) and  $m$  is the slope. The size modulus  $k$  can be expressed as  $\frac{X_0}{r}$  where  $X_0$  is the size of the initial particle and  $r$  is the size ratio.

The second equation was first developed empirically by Rosin and Rammuler<sup>(10)</sup> and then derived theoretically by Gilvarry<sup>(13)</sup>. It is

$$\frac{W(x)}{W_0} = 1 - e^{-\frac{x}{k}} \quad (3)$$

The symbols are the same as in equation 2. In this dissertation a third equation is derived. It is:

$$\frac{W(x)}{W_0} = 1 - \left(1 - \frac{x}{X_0}\right)^r \quad (4)$$

The exponent  $r$  is the size ratio.

All three equations are plotted in figure 1, on log-log paper. It is readily seen that if  $m$  in the Gaudin-Schuhmann equation is taken as 1, then all three equations converge to a straight line with a slope of 1 when  $x$  is small compared to  $X_0$ . If the straight line part of the curve is extrapolated to  $W/W_0 = 1$ , then the intersection  $\frac{x}{X_0} = \frac{1}{r}$ . This is the size ratio. Physically, it can be interpreted as the ratio of the size of the most prevalent weight fraction to the initial size. In other words, when a particle is broken, the greatest frequency of the mass appears at the size  $\frac{x}{X_0} = \frac{1}{r}$ . This definition is applicable only to single comminution events.



Size Frequency Distribution and Mass Frequency Distribution

In this section a model is proposed and from it a theoretical equation is derived which fits the experimental results better than equations (2) and (3).

The model of fracture is as follows: surfaces randomly oriented in position and direction pass through a crystal. The crystal fractures along segments of these surfaces. All fragments have the same shape.

The actual postulates made in the derivation may be stated as follows:

- 1) All fragments of the fractured crystal have the same shape.
- 2) Any characteristic dimension of the crystal, such as an edge or diagonal, which is cut by one of the randomly oriented surfaces is equi-likely to be cut anywhere along the line segment by that surface. The assumption that all fragments have the same shape puts constraints on how the surfaces cut the characteristic dimension in other directions. It is hoped that future work will uncover what restraints on the surfaces are involved to give a characteristic shape irrespective of size.

From these two postulates is derived a mathematical expression (see pp.12-19) which relates the distance along the characteristic dimension between two adjacent surfaces,  $\mu$ , and the frequency with which this distance  $\mu$  will occur. It is:

$$P_{\gamma}(\mu) = \frac{r}{X_0^r} (X_0 - \mu)^{r-1} d\mu \quad (5)$$

where  $P_{\gamma}(\mu)$  is the probability of the distance between two cuts being

exactly  $\mu$ ,  $r$  is the number of surfaces cutting the characteristic dimension of length  $X_0$ . The frequency distribution, corresponding to this probability is of course

$$f(\mu) = \frac{P_r(\mu)}{d\mu} = \frac{r}{X_0^r} (X_0 - \mu)^{r-1} \quad (6)$$

Equation 5 is used to derive the equation of cumulative weight finer versus size:

$$\frac{W(x)}{W_0} = 1 - \left(1 - \frac{x}{X_0}\right)^r \quad (4)$$

where  $x$  is the magnitude of the characteristic dimension of the fragment, such as the edge of a cube, and  $X_0$  is the magnitude of the characteristic dimension of the original particle.

Derivation of equation (5)

To derive equations 4 and 5, consider a line segment,  $X_0$  in length, cut by  $r$  surfaces. The object is to determine the frequency distribution of  $\mu$ , the distance between any two adjacent cuts.

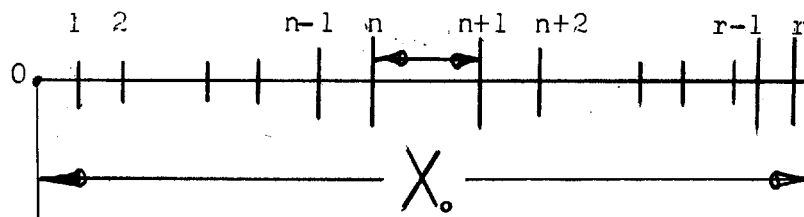


Figure A-1

Let there be  $r$  cuts along the line segment (figure A-1). The cuts

will be ordered by calling the one closest to the origin the first, the next, second, those to the last cut are called the  $r$ th cut. For the moment let the  $n$ th cut be fixed at  $X_n$  and the  $n + 1$ st cut be fixed at  $X_{n+1}$ . What is the probability that the  $n$ th and the  $n + 1$  cuts will be in a given position while there are  $(n - 1)$  cuts between 0 and the  $n$ th cut and  $r - (n + 1)$  cuts between the  $n + 1$  cut and  $X_0$ ?

Since the nomenclature used in this section is different from that of elementary texts in calculus, a brief explanation is included. Because this approach requires a large number of both variables and constants, subscripts are used to differentiate the variables as well as the constants. The lower case  $x$  denotes a variable, and the subscript denotes the cut with which the variable is associated. For example,  $x_i$  is the variable distance along the characteristic dimension to the  $i$ th cut. In figure A-1,  $x_{n-1}$  is the distance from the origin to the  $n - 1$  cut, which is not fixed. On the other hand, an upper case  $X$  such as  $X_0$  denotes a fixed distance.  $X_n$  is the distance, a constant distance, along the characteristic dimension to the  $n$ th cut, when and only when that cut remains fixed at a given point. The upper case  $P$  is used to denote a mathematical function of probability.  $P_i$  may or may not be related functionally to  $P_{i-1}$ .  $N(x,t)$  means that the function  $N(x,t)$  is a function of both  $x$  and  $t$ . The function  $N(x,t)$  is the same function as  $N(\gamma,t)$  but the variables are different. The nomenclature in this dissertation is similar to that used in Wadsworth's<sup>(14)</sup> book.

The probability of the  $n$ th cut being at a point  $X_n$  distant from the origin, is

$$\frac{dx_n}{X_0} \quad (7)$$

Similarly, the probability of the  $n + 1$  cut being at  $X_{n+1}$  is:

$$\frac{dx_{n+1}}{X_0} \quad (8)$$

The probability of having  $n - 1$  cuts between 0 and  $X_n$  is:

$$\left(\frac{X_n}{X_0}\right)^{n-1} \quad (9)$$

and similarly, the probability of having  $r - (n + 1)$  cuts above  $X_{n+1}$  is

$$\left[\frac{X_0 - X_{n+1}}{X_0}\right]^{r-n-1} \quad (10)$$

The probability,  $P_{1-4}^{(X_n, X_{n+1})}$  of having all of these events happen simultaneously is the product of their individual probabilities

$$P_{1-4}^{(X_n, X_{n+1})} = \frac{(X_n)^{n-1}}{(X_0)^{n-1}} \frac{dx_n}{X_0} \frac{dx_{n+1}}{X_0} \frac{(X_0 - X_{n+1})^{r-n-1}}{X_0^{r-n-1}} \quad (11)$$

Equation 11 gives the probability that there will be  $n - 1$  cuts between 0 and  $X_n$ , one cut at  $X_n$ , one cut at  $X_{n+1}$ , and  $r - n - 1$  cuts between  $X_n$  and  $X_0$ . Since the  $r$  cuts were ordered after the event took place, a multinomial coefficient must be used to determine all possible ways  $r$  cuts can cut a line with only the  $n$ th, and  $n + 1$ st cut having a fixed position. Since there are two groups of cuts,  $n - 1$  below  $X_n$  and  $r - n - 1$

above  $X_{n+1}$  the multinomial coefficient,  $\alpha$ , is:

$$\alpha = \frac{r!}{(n-1)!(r-n-1)!} \quad (12)$$

Thus the probability,  $P_5(X_n, X_{n+1})$  of having  $r$  cuts at random on a line segment,  $X_0$  in length, with the  $n$ th and  $n+1$ st cuts fixed is  $\alpha P(X_n, X_{n+1})$ .  
1-4

Thus

$$P_5(X_n, X_{n+1}) = \frac{r!}{(n-1)!(r-n-1)!} \frac{X_n^{n-1}}{X_0^r} (X_0 - X)^{(r-n-1)} dx_n dx_{n+1} \quad (13)$$

What is of interest is the distribution of the distance between the  $n$ th and the  $n+1$ st cuts. Let  $\mu$  be the distance between the two cuts. At this point, the position of the  $n$ th and  $n+1$ st cuts are allowed to vary, that is  $X_n$  becomes  $x_n$ ,  $X_{n+1}$  becomes  $x_{n+1}$ , and

$$\mu = x_{n+1} - x_n \quad (14)$$

Rearranging

$$x_{n+1} = \mu + x_n \quad (15)$$

The first step, after Wadsworth<sup>(15)</sup>, in deriving the distribution of  $\mu$  is to regard  $x_n$  as fixed while  $x_{n+1}$  varies. The derivative of  $x_{n+1}$  with respect to  $\mu$  holding  $x_n$  fixed will be a partial derivative. Thus,

$$\frac{\partial x_{n+1}}{\partial \mu} = 1 \quad (16)$$

The joint distribution of  $\mu$  and  $x_n$  is given by equation 13, where

$0 \leq \mu \leq X_0 - x_n$ . Substituting the values of equation 16 and 15 into equation 13

$$P_6(\mu, x_n) = \alpha (X_0)^{-r} (x_n)^{n-1} (X_0 - \mu - x_n)^{r-n-1} d\mu dx_n \quad (17)$$

Since this equation contains both  $\mu$ , the desired variable, and  $x_n$ , the equation will be integrated with respect to  $x_n$  to eliminate it. This can be done because equation 17 is a joint distribution of two independent variables. By integrating one of the variables between its limits, the individual distribution of the other is obtained. The lower limit of  $x_n$  is zero.

$$x_n \geq 0 \quad (18)$$

The upper limit of  $x_n$  is fixed by equation 14 for when  $x_{n+1}$  is at its maximum:

$$x_n \leq X_0 - \mu \quad (19)$$

Integrating equation 17 and putting in the limits for  $x_n$

$$P_7(\mu) = \alpha X_0^{-r} \int_0^{X_0 - \mu} (x_n)^{n-1} ((X_0 - \mu) - x_n)^{r-n-1} dx_n \quad (20)$$

The form of the integral can be changed by defining a new variable  $y$  such that

$$x_n = y (X_0 - \mu) \quad (21)$$

$$dx_n = (X_0 - \mu) dy \quad (22)$$

Substituting the values of  $x_n$  from equation 21 and 22 into equation 17

$$P_7(\mu) = \alpha X_0^{-r} (X_0 - \mu)^{r-1} \int_0^1 y^{n-1} (1-y)^{r-n-1} dy \quad (23)$$

The integral in the equation is a beta function

$$\int_0^1 y^{n-1} (1-y)^{r-n-1} dy = \beta(n, r-n) \quad (24)$$

This beta function can be expressed in terms of gamma functions

$$\beta(n, r-n) = \frac{\Gamma(n) \Gamma(r-n)}{\Gamma(r)} \quad (25)$$

Since both  $r$  and  $n$  are integers:

$$\frac{\Gamma(n) \Gamma(r-n)}{\Gamma(r)} = \frac{(n-1)! (r-n-1)!}{(r-1)!} \quad (26)$$

Thus the integral of equation 24 equals

$$\int_0^1 y^{n-1} (1-y)^{r-n-1} dy = \frac{(n-1)! (r-n-1)!}{(r-1)!} \quad (27)$$

Substituting the results of equation 27 into 23

$$P_7(\mu) = \frac{r}{X_0^r} (X_0 - \mu)^{r-1} d\mu \quad (28)$$

Equation 28 is identical with equation 5.

Equation 28 can be interpreted as follows.  $P_7(\mu)$  is the probability of obtaining a distance of exactly  $\mu$  between two adjacent cuts. Though the equation was derived by considering the distance between the  $n$ th and  $n+1$ st cut,  $n$  does not appear as a parameter in the final equation. Actually this is not strictly true in this case, for the deriva-

tion of  $P_7(\mu)$  was for one specific line. Once the distance between two cuts has been fixed then all the other  $r - 2$  cuts must fall within a distance  $X_0 - \mu$ . However, if one considers what happens when a large number of particles are broken then this restriction is removed. Thus  $\mu$  may be regarded as the distance between any two adjacent cuts regardless of where the cuts were. This is significant for it simplifies the mathematics.

A relatively simple check can be made on equation 28 to see that it is a distribution function. The probability of  $\mu$  being between 0 and  $X_0$  is 1, because the distance between two adjacent cuts must be equal to or greater than zero but equal to or less than the length of the line being cut,  $X_0$ . Therefore, the integrand of equation 28 between 0 and  $X_0$  must be 1.

$$\int_0^{X_0} P_7(\mu) = \frac{r}{X_0^r} \int_0^{X_0} (X_0 - \mu)^{r-1} d\mu \quad (29)$$

Let

$$w = (X_0 - \mu) \quad (30)$$

Thus

$$dw = -d\mu \quad (31)$$

Substituting equation 30 and 31 into 29

$$\int_0^{X_0} P_7(\mu) = \frac{-r}{X_0^r} \int_{X_0}^0 w^{r-1} dw \quad (32)$$



$$\int_0^{X_0} P_7(\mu) = + \frac{r}{X_0^r} \frac{X_0^r}{r} = 1 \quad (33)$$

This shows that equation 28 has the property of a distribution function.

Derivation of CWF equation (equation 4)

From equation 28 it is possible to derive an equation for CWF.

The relative volume of a fragment of characteristic size  $\mu$  and one of the original size  $X_0$  is  $(\frac{\mu}{X_0})^3$ . Hence the abundance  $S(\mu)$  of particles of size  $\mu$  equals the probability of fracture pieces being of that size, given by equation 28 divided by the relative volume  $(\frac{\mu}{X_0})^3$ , or

$$S(\mu) = \frac{X_0^3}{\mu^3} \frac{r}{X_0^r} (X_0 - \mu)^{r-1} d\mu \quad (34)$$

The mass of particles of size  $\mu$ ,  $M(\mu)$ , is obtained by multiplying the number of particles of size  $\mu$  by the mass of each particle  $\lambda \rho \mu^3$

$$M(\mu) = S(\mu) \lambda \rho \mu^3 = \lambda \rho \frac{X_0^3}{X_0^r} r (X_0 - \mu)^{r-1} d\mu \quad (35)$$

In this equation  $\rho$  stands for the density of the particles and  $\lambda$  for the shape factor such that

$$V = \lambda \mu^3 \quad (36)$$

where  $V$  is the volume of the particle having a characteristic size  $\mu$ .

$M(\mu)$  can be interpreted as being the infinitesimal mass of fragments having exactly this size  $\mu$ . Normally the integral of this expression is used in presenting data. If the integral is between 0 and a given size  $x$ , it is called the CWF plot. If on the other hand, it is between  $x_1$  and  $x_2$  where  $x_1$  and  $x_2$  may be two seriated screen sizes, then it is the weight retained equation. Since most data in the literature are presented in terms of CWF plot, the integral from 0 to  $x$  will be used.

The integral of  $M(\mu)$  is defined as  $W(x)$  in the following manner:

$$W(x) = \int_0^x M(\mu) d\mu \quad (37)$$

After differentiating

$$dW(\mu) = M(\mu) d\mu \quad (38)$$

Substituting the value of  $M(\mu)$  obtained in equation 35

$$dW(\mu) = \frac{\lambda \rho x_0^3}{x_0^r} r (x_0 - \mu)^{r-1} d\mu \quad (39)$$

Setting up the integral between the limits of 0 and  $x$

$$W(x) = \frac{\lambda \rho x_0^3}{x_0^r} r \int_0^x (x_0 - \mu)^{r-1} d\mu \quad (40)$$

On completing the integration, inserting limits, and simplifying:

$$W(x) = \lambda \rho X_0^3 \left( 1 - \left( 1 - \frac{x}{X_0} \right)^r \right) \quad (41)$$

The weight of the original crystal is  $\lambda \rho X_0^3$  where  $X_0^3$  is the cube of the characteristic dimension,  $\lambda$  is a dimensionless number which corrects for the shape factor to give the true volume and  $\rho$  is the density.

$$W_0 = \lambda \rho X_0^3 \quad (42)$$

Substituting this result in equation <sup>41</sup>42

$$\frac{W(x)}{W_0} = 1 - \left( 1 - \frac{x}{X_0} \right)^r \quad (43)$$

#### Comparison of this CWF equation with other equations

Equation 43 is the same as equation 4. All that remains is to compare it to the Gaudin-Schuhmann and the Gilvarry equation. Let:

$$X_0 = rK \quad (44)$$

where  $K$  is a constant to be defined later.

Substituting this value of  $X_0$  in equation 43

$$\frac{W}{W_0} = 1 - \left( 1 - \frac{x}{rK} \right)^r \quad (45)$$

Expand the righthand side of equation 45 by the binomial theorem.

$$\frac{W}{W_0} = \frac{x}{K} - \frac{r(r-1)}{r^2 2!} \left( \frac{x}{K} \right)^2 + \frac{r(r-1)(r-2)}{r^3 3!} \left( \frac{x}{K} \right)^3 \quad (46)$$

Dropping all but the first term

$$\frac{W}{W_0} = \frac{x}{K} \quad (47)$$

Hukki<sup>(5)</sup> found that  $m$ , the slope of equation 2 was one for a single comminution event. Consequently, equation 2 and equation 47 are equivalent if:

$$K = k, \quad (48)$$

that is if the constant  $K$  introduced in equation 44 is the modulus of the product.

Charles defines reduction ratio,  $R$ , as the modulus of the feed,  $k_f$ , divided by the modulus of the product,  $k_p$ ,

$$R = \frac{k_f}{k_p} \quad (49)$$

In the case of single comminution event this is

$$R = \frac{X_o}{K} \quad (50)$$

By virtue of equations 45, 49 and 50,  $r$  is similar to the reduction ratio

$$r = R = \frac{X_o}{k} \quad (51)$$

The significance of equation 52 is that  $r$ , the number of surfaces cutting the characteristic dimension is similar to the reduction ratio,  $R$ , and the size modulus  $k$  is equivalent to  $\frac{X_o}{r}$  in the case of a single comminution event. This equivalence is true only when the size ratio is greater than 1.

Equation 45 may be rewritten so that:

$$\frac{W_o - W(x)}{W_o} = \left(1 - \frac{x}{rk}\right)^r \quad (52)$$

Now, define  $Q$  as the cumulative weight of material greater than a given size  $x$ . Thus:

$$Q = W_0 - W(x) \quad (53)$$

Substituting the value for  $Q$  in equation 52

$$\frac{Q}{W_0} = \left(1 - \frac{x}{rk}\right)^r \quad (54)$$

Equation 54 is the alternate method of presenting 45. These two equations both describe the size distribution to be expected from the fracture of a single, homogeneous crystal. It is of interest that the slope of equation 47 which is the approximation of equation 45 has a slope of 1. This is the experimental verification of Hukki's<sup>(5)</sup> contention that the slope of the fracture of a single crystal is one.

Gilvarry<sup>(13)</sup>, by considering edge flaws has derived an equation which is similar to the Gaudin-Schuhmann equation. Using the same nomenclature, the Gilvarry equation is:

$$\frac{W(x)}{W_0} = 1 - e^{-x/k} \quad (55)$$

Expanding and dropping the higher order terms of  $\left(\frac{x}{k}\right)$  this equation becomes

$$\frac{W(x)}{W_0} = \frac{x}{k} \quad (56)$$

This is the same as equation 47 and approximates equation 2 if the slope,  $m$ , equals one. Equation 55 generally approximates equation 43 except that it is for the largest size ranges.

Unfortunately, the Gilvarry equation does not conserve mass, for

in the interval between 0 and  $X_0$  the fraction of the mass,  $(\frac{W}{W_0})$ , is less than 1 for all finite values of  $x$ . This means that particles larger than the original must be considered if the mass is to be conserved. This appears to be a contradiction of the boundary condition.

The Gaudin-Schuhmann equation, while conserving the mass at finite sizes, has never fitted the experimental data in the upper size ranges.

## REPEATED FRACTURE

Repeated fracture is the sum of a series of individual, sequential comminution events. In repeated fracture both the initial particles and their daughter fragments are broken. It is as if a drinking glass were broken on the floor and then a hammer were used to pulverize the fragments.

In a ball mill, large particles are broken and fragments of the large particles are again broken in later, individual comminution events. This is the way which almost all commercial comminution devices operate. In this section a method for predicting the results of repeated comminution of homogeneous solids will be proposed. A mathematical model will be set up. Analytical and numerical solutions will be given in the section on results.

As delineated in the section on Single Fracture a single comminution event produces a mass frequency distribution. Likewise, the sum of a series of individual comminution events will produce a mass frequency distribution. If one knows the input to a comminution device and the particles which have been comminuted, one can predict the output mass frequency distribution.

For example, if the input were two water tumblers, both of which were broken on the floor and the pieces larger than one inch were broken with a hammer, then the output mass frequency distribution could be predicted. One only need know the input and what transpired to predict the output.

The model of repeated fracture presented consists of three parts:

the concept of the half-life of a particle, how the half life varies with time; and the size ratio of an individual particle when it is fractured. Experimentally, each of these three parts can be measured independently of the other two.

The concept of half-life of radio isotopes is clearly established. The concept of half-life of a particle in a ball mill is essentially the same. If one starts out with 100 particles of a given size, how long is it until only 50 of the original particles remain? That length of time is called the half-life. It is assumed that the half-life does not vary with time.

As the half-life of radio isotopes varies from isotope to isotope so one would expect the half-life to vary with the size of the particle. It is possible to derive how the half-life of a particle will vary in rod mills and in ball mills.

The basic assumption made is that the probability of a particle being broken is independent of the mill loading. That is to say, if a particle is in the path of a descending ball it will be broken irrespective of the number of other particles in the path of a descending ball.

If a particle, assumed to be a sphere, of radius  $x$  is to be broken by a ball of radius  $R$ , then the particle must be within a radius  $y$  of the contact point of the ball and mill. See Figure A-2. Consider now the line running from the center of the ball to the center of the sphere. Its length is  $R + x$ . Consider now a perpendicular projection of the center of the particle on the vertical radius of the ball. Call this point,



P. The distance  $\overline{OP}$  is  $(R - x)$  in length. By simple geometry

$$(R + x) \cos \theta = (R - x) \quad (57)$$

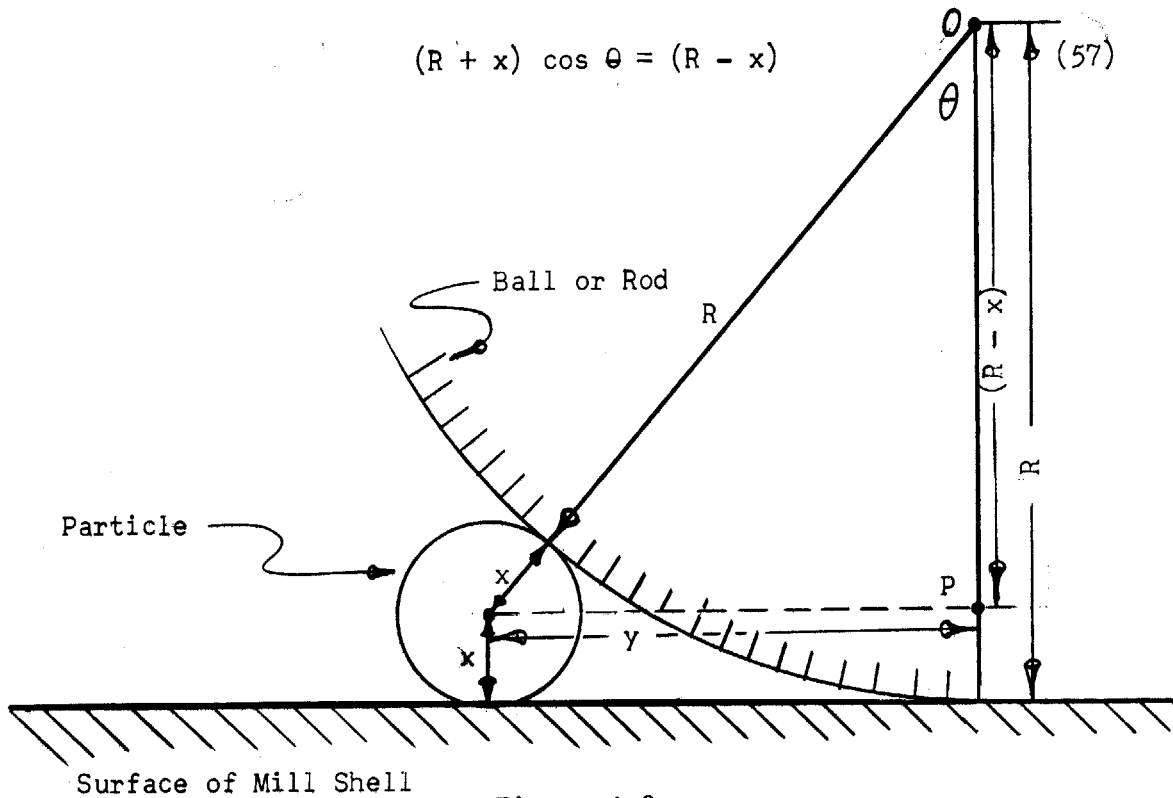


Figure A-2

Dividing by  $(R + x)$

$$\cos \theta = \frac{R - x}{R + x} \quad (58)$$

By definition of a sine and the Pythagorean theorem

$$\sin \theta = \sqrt{\frac{(R + x)^2 - (R - x)^2}{(R + x)^2}} \quad (59)$$

*Spelling*

Collecting terms

$$\sin \theta = \frac{2}{R + x} \sqrt{Rx} \quad (60)$$

Referring to Figure A-2

$$y = (R + x) \sin \theta \quad (61)$$

Substituting the value for  $\sin \theta$  obtained in equation 60

$$y = 2\sqrt{Rx} \quad (62)$$

This is an exact derivation. Equation 62 may be written

$$y = (2\sqrt{R}) \sqrt{x} \quad (63)$$

The results obtained in equation 63 are also obtained if one considers the case of a ball in a large cylindrical mill. Figure A-3 or the collision of two balls, Figure A-4. Naturally the constant in

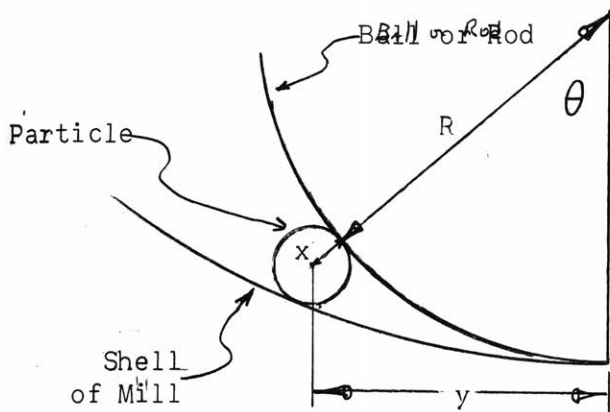


Figure A-3

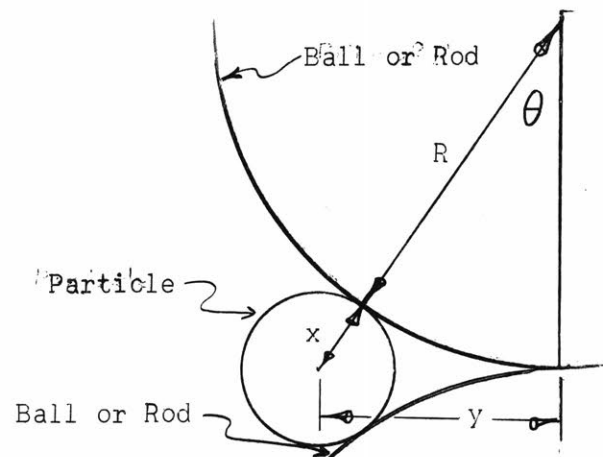


Figure A-4

front of the  $\sqrt{x}$  differs in each case. Equation 62 and 63 are equally valid for rods in a rod mill, providing the axis of the cylinders are parallel.

The question to be settled is: how does the probability of a particle being broken vary with the size of the particle? In a ball mill, all particles within a radius  $y$ , see Figure A-2, will be broken. Thus the probability is:

$$P = \frac{\pi y^2}{A_m} \quad (64)$$

Where  $A_m$  is the area of the mill.

Substituting the value of  $y$  from equation 63

$$P = \frac{4\pi Rx}{A_m} \quad (65)$$

Since the radius of the ball,  $R$ , and the area of the mill,  $A_m$ , are constant, the probability can be expressed as:

$$P = c_1 x \quad (66)$$

where  $c_1$  is a constant. The conclusion is that the probability of breakage of a particle in a ball mill is proportional to the first power of the radius of the particle.

In a rod mill, all particles within a distance  $y$  of the center line of contact will be broken. Thus, for a unit length,  $L$ , of rod the probability of a particle being broken is:

$$P = \frac{2Ly}{A_m} \quad (67)$$

Substituting the value of equation 63

$$P = \frac{4L\sqrt{Rx}}{A_m} \quad (68)$$

Since  $A_m$ ,  $R$  and  $L$  are constant, equation 68 may be expressed as

$$P = c_2 \sqrt{x} \quad (69)$$

where  $c_2$  is a constant. In a rod mill, the probability of a particle being broken varies with the square root of particle size. This is

very different from the ball mill where the probability of being broken varies with the first power of particle size.

The results of this analysis suggest that the rod mill does more grinding of fine particles than does a ball mill. Thus one would expect that when attempting to grind a material a rod mill would be used first for general grinding followed by a ball mill for selective grinding of the larger particle. In practice a ball mill is generally used after a rod mill, but for other reasons than more selective grinding of the larger particles. No doubt there are factors not considered here that intervene.

A stamp mill can be analyzed in a similar manner. A flat bottomed plunger strikes the material on a flat plate. The probability of being broken,  $P(x)$ , is equal to a constant. Thus it can be said that  $P(x) = cx^0$ . In this equation the exponent of  $x$  has the value zero.

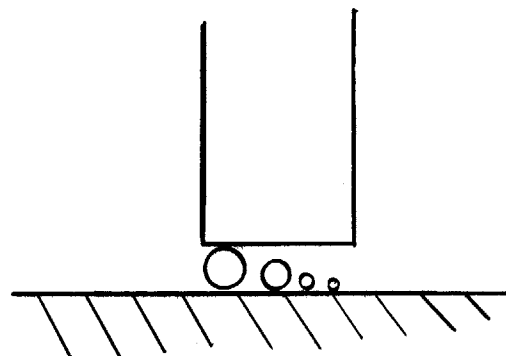


Figure A-5

In general, one would expect that the probability of grinding would have an equation of the form:

$$P = c x^g \quad (70)$$

where  $g$ , a dimensionless exponent, has a value between 0 and 1 or perhaps 2, and depends on the comminution device.

## A MATHEMATICAL MODEL OF REPEATED FRACTURE

With the development of the CWF equation for single fracture and the development of  $P(x)$  for particle size, it is now possible to derive an equation which expresses the CWF for repeated fracture. This CWF equation is a function of both time and size. The solution of the equation appears later in the text.

To develop the mathematical model, a mass balance is made on the number of particles of exactly size  $x$ . The number of particles of size,  $x$ , at time,  $t$ , is defined as  $N(x,t)$ . The instantaneous change in the number of particles,  $\frac{\partial N(x,t)}{\partial t}$  must be equal to the number of particles entering the  $x$  size range, as fragments of larger particles, minus the number of particles leaving the size range because they are broken. This can be expressed as an equation:

$$\frac{\partial N(x,t)}{\partial t} = \text{particles entering} - \text{particles leaving} \quad (71)$$

The number of particles leaving the size range  $x$  is equal to the probability of any one particle leaving per unit time,  $P(x)$ , times the number of particles in that particular size range,  $N(x,t)$ . Therefore equation 71 can be written:

$$\frac{\partial N(x,t)}{\partial t} = \text{particles entering} - P(x)N(x,t) \quad (72)$$

It should be noted that the probability of a particle leaving a given size range does not vary with time.

The number of particles entering the size range,  $x$ , is a little

more complicated. In order for a particle to enter size  $x$  it must be a fragment of a larger particle which is broken. Let  $\gamma$  denote the size of the larger particle. The probability of a larger particle being broken in a given length of time  $\Delta t$  is  $P(\gamma)$  and the number of particles of size  $\gamma$  at time,  $t$ , is by definition  $N(\gamma, t)$ . Therefore the number of particles of exactly size  $\gamma$  being broken in  $\Delta t$  is  $P(\gamma)N(\gamma, t)$ . Equation 34 expresses the relative abundance of particle,  $S(\mu)$ , as a function of initial particle size and reduction ratio. The equation may be written

$$S(x) = \frac{\gamma^3}{x^3} \frac{r}{\gamma^r} (\gamma - x)^{r-1} dx \quad (73)$$

This equation is comprised of two parts: the infinitesimal,  $dx$ , and the frequency,  $\frac{\gamma^3}{x^3} \frac{r}{\gamma^r} (\gamma - x)^{r-1}$  of a particle of size  $x$  occurring;

this might be termed  $f(x)$ . Actually  $f(x)$  is the frequency which a fragment of size  $x$  occurs when a particle of size  $\gamma$  is broken with a size ratio of  $r$ . By multiplying the number of particles of size  $\gamma$  being broken by the frequency of occurrence of fragments of size  $x$  formed by the fracture of a particle of size  $\gamma$  gives the number of particles of size  $x$  formed by the fracture of  $P(\gamma)N(\gamma, t)$  particles. It is  $P(\gamma)N(\gamma, t) f(x)$ . This, however, is only the number of fragments of  $x$  formed by the fracture of particles of exactly size  $\gamma$ . Since  $\gamma$  can be any particle size greater than  $x$  but equal to or less than  $X_0$ , the largest initial particle, then, to obtain the total num-

ber of fragments of size  $\gamma$  one must integrate the expression from  $x$  to  $X_0$ . In other words,  $x \leq \gamma \leq X_0$  and thus the total number of particles breaking into fragments of size  $x$  in time  $\Delta t$  is the integral of  $\gamma$  from  $\gamma = x$  to  $\gamma = X_0$ . It is:

$$\text{no. of fragment of size } x = \int_x^{X_0} P(\gamma)N(\gamma,t) \frac{\gamma^3}{x^3} \frac{r}{\gamma^r} (\gamma - x)^{r-1} d\gamma \quad (74)$$

Substituting this result in equation 72:

$$\frac{\partial N(x,t)}{\partial t} = -P(x)N(x,t) + \int_x^{X_0} P(\gamma)N(\gamma,t) \frac{\gamma^3}{x^3} \frac{r(\gamma - x)^{r-1}}{\gamma^r} d\gamma \quad (75)$$

Note that the integral is on  $\gamma$ , not  $x$ .

This equation can be put in a more manageable form if equation 75 is multiplied by  $\rho\lambda x^3$ :

$$\frac{\partial}{\partial t} [\rho\lambda x^3 N(x,t)] = -P(x) [\rho\lambda x^3 N(x,t)] + \int_x^{X_0} P(\gamma) [\rho\lambda \gamma^3 N(\gamma,t)] \frac{r(\gamma-x)^{r-1}}{\gamma^r} d\gamma \quad (76)$$

The number of particles of a given size  $x$ ,  $N(x,t)$ , times the mass of a particle of size  $x$ ,  $\rho\lambda x^3$ , is the mass of particles,  $M(x,t)$  of size  $x$ . Substituting this in equation 76

$$\frac{\partial M(x,t)}{\partial t} = -P(x)M(x,t) + \int_x^{X_0} P(\gamma)M(\gamma,t) \frac{r(\gamma-x)^{r-1}}{\gamma^r} d\gamma \quad (77)$$

This integral-differential equation is valid for comminution devices so long as the  $P(x)$ , the probability of a particle being broken, does not vary with time. Unfortunately, analytical solutions have not been found for equation 77, except in very special cases. It can be solved numerically however. The analytical and numerical solutions follow.



## ANALYTICAL SOLUTIONS TO EQUATION 77

Equation 77 can be solved under special circumstances. Two such solutions are presented below.

1) Decay of feed size material in product.

Consider the case where all the material is initially of size  $X_0$ . Since there is no material larger than  $X_0$ , the amount of material entering from a larger size range is zero. Thus equation 77 becomes:

$$\frac{\partial}{\partial t} M(X_0, t) = - P(X_0) M(X_0, t) \quad (78)$$

Since  $X_0$  is a constant, this equation is equivalent to

$$\frac{dM(X_0, t)}{dt} = - P(X_0) M(X_0, t) \quad (79)$$

Separating the variables

$$\frac{dM(X_0, t)}{M(X_0, t)} = - P(X_0) dt \quad (80)$$

Integrating

$$\underline{\text{Log } M(X_0, t)} = - P(X_0)t + \text{Const} = - P(X_0)t + \log f(X_0) \quad (81)$$

$$M(X_0, t) = f(X_0) e^{-P(X_0)t} \quad (82)$$

When  $t = 0$

$$M(X_0, t) = M(X_0, 0) \quad (83)$$

hence, from equation 82:

$$M(X_0, 0) = f(X_0) \quad (84)$$

Consequently equation 82 becomes:

$$M(X_0, t) = M(X_0, 0)e^{-P(X_0)t} \quad (85)$$

The amount of initial material of size  $X_0$ ,  $M(X_0, 0)$  is a constant,  $M_0$

$$M(X_0, 0) = M_0 \quad (86)$$

Thus equation 85 becomes:

$$M(X_0, t) = M_0 e^{-P(X_0)t} \quad (87)$$

Equation 87 predicts an exponential decay of the material in a given size fraction, if no new material is entering that size range.

A very similar example is where the material in a given size fraction is tagged either chemically or radioactively.<sup>(16)</sup> Since the material is tagged for one, given size fraction, no new, tagged material can break into that size fraction. Consequently, the tagged material which remains in that size fraction is also predicted by equation 87.

## 2) General solution for fixed values of parameters

Consider the case where:

i  $P(x) = +cx$ ,  $c$  being a constant

ii  $r = 1$

Equation 77 becomes

$$\frac{\partial}{\partial t} M(x, t) = -cxM(x, t) + c \int_x^{X_0} M(\gamma, t) d\gamma \quad (88)$$

let:

$$R(x,t) = + c \int_x^{X_0} M(\gamma,t) d\gamma \quad (89)$$

Differentiating 89 with respect to x

$$- \frac{\partial}{\partial x} R(x,t) = cM(x,t) \quad (90)$$

In this differentiation, <sup>(17)</sup> note that the limits between which  $M(\gamma,t)$  is integrated affect variables in the derivative.

Substituting equation 89 and 90 into 88:

$$\frac{1}{c} \frac{\partial^2}{\partial x \partial t} R(x,t) = - x \frac{\partial}{\partial x} R(x,t) - R(x,t) \quad (91)$$

This is equal to:

$$\frac{\partial^2}{\partial t \partial x} R(x,t) = - \frac{c \partial}{\partial x} [xR(x,t)] \quad (92)$$

Integrating both sides with respect to x:

$$\frac{\partial}{\partial t} R(x,t) = - cxR(x,t) \quad (93)$$

Divide by  $R(x,t)$ :

$$\frac{\frac{\partial}{\partial t} R(x,t)}{R(x,t)} = - cx \quad (94)$$

Integrate with respect to t:

$$\log R(x,t) = - cxt + h(x) \quad (95)$$

in which  $h(x)$  is an arbitrary function.

Anti logging:

$$R(x,t) = g(x)e^{-cxt} \quad (96)$$

$g(x)$  is an arbitrary function which is the anti log of  $h(x)$ .

From equation 89:

$$R(X_0,t) = 0 \quad (97)$$

for all values of  $t$ . Hence

$$g(X_0) = 0 \quad (98)$$

Equation 96 is the general solution of equation 93. Thus from 89 and 96

$$c \int_x^{X_0} M(\gamma,t) d\gamma = g(x)e^{-cxt} \quad (99)$$

Differentiating

$$-M(x,t) = \frac{e^{-cxt}}{c} \left[ \frac{\partial}{\partial x} g(x) - ct g(x) \right] \quad (100)$$

Initially

$$M(x,0) = f(x) \quad (101)$$

At time  $t = 0$ , equation 100 becomes

$$M(x,0) = - \frac{\partial}{\partial x} \frac{g(x)}{c} \quad (102)$$

Thus

$$\frac{\partial}{\partial x} g(x) = - cf(x) \quad (103)$$

If  $g(x)$  is defined in the following manner

$$g(x) = c \int_x^{X_0} f(\gamma) d\gamma \quad (104)$$

When  $x = X_0$  then:

$$g(X_0) = 0 \quad (105)$$

This conforms to equation 98. Equation 100 becomes

$$M(x,t) = e^{-cxt} \left[ ct \int_x^{X_0} f(\gamma) d\gamma + f(x) \right] \quad (106)$$

A critical test of equation 106 is the conservation of mass for all  $t$ . Substituting equation 89 into 96 and setting  $x = 0$

$$-R(0,t) = c \int_0^{X_0} M(\gamma,t) d\gamma = g(0) \quad (107)$$

From equation 104

$$g(0) = \int_0^{X_0} f(\gamma) d\gamma \quad (108)$$

The integral of  $f(x)$  from 0 to  $X_0$  is the initial mass,  $M_0$ . From equation 107 and 108

$$\int_0^{X_0} M(\gamma,t) d\gamma = \int_0^{X_0} f(\gamma) d\gamma = M_0 \quad (109)$$

Since  $M(x,t)$  is a function of  $x$  and  $t$  and the integral over all  $x$  is constant for any  $t$ , then the mass is conserved for all time,  $t$ .

Equation 106 expresses the mass frequency distribution as a function of both time and size. It does so for any initial input. The conditions chosen are those of a ball mill. The restriction that the size ratio is equal to 1,  $r = 1$ , is severe. However, equation 106 does show how a solution would be expected to behave if analytical solutions could be obtained. One of the outstanding characteristics of the equation is the exponential decay that the term  $e^{-cxt}$  imposes on the equation. The other feature is that the term  $ct \int_0^{X_0} f(\gamma) d\gamma$  will, at first, cause an increase in the material in a given size range  $x$  but the exponential multiplier eventually causes the material in size range  $x$  to decrease and vanish. It is important to remember, however, that the mass is conserved at all times.

Equation 77 has been solved numerically for a number of values of  $r$  and  $P(x)$ . To compare the numerical solution with the one derived in this section, set

$$\int_0^x f(x) dx = \begin{cases} U_0 & x = X_0 \\ 0 & x < X_0 \end{cases} \quad (110)$$

In other words, the integral of the function  $f(x)$  is zero for  $x$  less than  $X_0$ , and is equal to  $U_0$  for  $x = X_0$ . Essentially the integral of  $f(x)$  is a step function.

The form in which the numerical data is plotted is weight retained between two different screen sizes. The screen size openings vary by a ratio of 2. In terms of  $R(x,t)$  this is:

$$U(x,t) = R(2x,t) - R(x,t) \quad (111)$$

From equation 89, 106, 109 and 110

$$U(x,t) = e^{-cxt} \int_{x_0}^{X_0} f(\gamma) d\gamma - e^{-2cxt} \int_{2x}^{X_0} f(\gamma) d\gamma \quad (112)$$

$$U(x,t) = \begin{cases} U_0 [e^{-cxt} - e^{-2cxt}] & x < X_0 \\ U_0 e^{-ctx} & x = X_0 \end{cases} \quad (113)$$

dividing by  $U_0$

$$\frac{U(x,t)}{U_0} = \begin{cases} e^{-cxt} - e^{-2ctx} & x < X_0 \\ e^{-cxt} & x = X_0 \end{cases} \quad (114)$$

Solving for a maximum value of  $U(x,t)$  with respect to  $x$ .

$$\frac{dU(x,t)}{dx} = 0 = -cte^{-ctx} + 2cte^{-2ctx} \quad (115)$$

Dividing by  $ct$ , multiplying by  $e^{+2ctx}$  and transposing

39.

$$e^{+ctx} = 2 \quad (116)$$

Logging and solving for x

$$x = \frac{1}{ct} \ln 2 = \frac{.693}{ct} \quad (117)$$

Substituting this in equation 114 the maximum value of  $U(x,t)$  is

$$U_{\max}(x,t) = .25 \text{ at } x = \frac{1.386}{t} \quad (118)$$

if  $c = 1/2$ .



METHOD OF NUMERICAL SOLUTION OF EQUATION 77

Since equation 77 can only be solved in certain specific cases, numerical methods must be used for a wider variety of solutions. The grinding process is considered a Markov chain and solved as such for various times.

Equation 77 is the basic equation to be solved and is:

$$\frac{\partial M(x,t)}{\partial t} = -P(x)M(x,t) + \int_x^{X_0} P(\gamma)M(\gamma,t) \frac{r(\gamma-x)^{r-1}}{\gamma^r} d\gamma \quad (119)$$

If small increments of time,  $\Delta t$ , are taken  $\frac{\partial}{\partial t} M(x,t)$  can be approximated by

$$\frac{\partial}{\partial t} M(x,t) = \frac{\Delta M(x,t)}{\Delta t} \quad (120)$$

$\frac{\Delta M(x,t)}{\Delta t}$  can be represented as:

$$\frac{\Delta M(x,t)}{\Delta t} = M(x,t_{n+1}) - M(x,t_n) \quad (121)$$

Where:

$$\Delta t = t_{n+1} - t_n = 1 \quad (122)$$

Hence, equation 119 can be written as:

$$M(x,t_{n+1}) - M(x,t_n) = -P(x)M(x,t_n) + \int_x^{X_0} P(\gamma)M(\gamma,t_n) \frac{(\gamma-x)^{r-1}}{\gamma^r} d\gamma \quad (123)$$

Rearranging terms:

$$M(x, t_{n+1}) = [1 - P(x)] M(x, t_n) + \int_x^{X_0} P(\gamma) M(\gamma, t_n) r \frac{(\gamma - x)^{r-1}}{\gamma^r} d\gamma \quad (124)$$

Attempts to develop a difference equation from equation 77 were unsuccessful. However, this equation can readily be expressed by a Markov chain. It is not the purpose of this dissertation to develop the use of Markov chains or matrix algebra. The reader is referred to books by Feller<sup>(18)</sup> and Hildebrand<sup>(19)</sup>. However, a brief explanation will be given. The matrix below is an  $m$  by  $m$  matrix. There are  $m$  rows and  $m$  columns. All matrices in this dissertation are 20 by 20.

	<u>Column</u>			
<u>Row</u>	1	2	3	$m$
1	$a_{11}$	$a_{12}$	$a_{13}$	$a_{1m}$
2	$a_{21}$	$a_{22}$	$a_{23}$	$a_{2m}$
$m$	$a_{m1}$	$a_{m2}$	$a_{m3}$	$a_{mm}$

See Fig. A-6. Each position in the matrix is designated by a coefficient with 2 subscripts,  $a_{ij}$ . The first subscript designates the row, and the second subscript designates the column. For example, the coefficient  $a_{26}$  is the coefficient in the second row and the sixth column.

To make a Markov matrix to represent equation 124, the largest size fraction of material is designated  $m$ . The size fraction  $m$  means all material in the size range of  $\frac{X_0}{2}$  to  $X_0$ . Likewise the size fraction  $m-1$

MARKOV T=1 P=0.5XE1 R=8			COL. 3	COL. 4	COL. 5	COL. 6	COL. 7	COL. 8	COL. 9	COL. 10	COL. 11	COL. 12	COL. 13	COL. 14	COL. 15	COL. 16	COL. 17	COL. 18	COL. 19	COL. 20
ROW	COL. 1	COL. 2	COL. 3	COL. 4	COL. 5	COL. 6	COL. 7	COL. 8	COL. 9	COL. 10	COL. 11	COL. 12	COL. 13	COL. 14	COL. 15	COL. 16	COL. 17	COL. 18	COL. 19	COL. 20
ROW 1	1.00000E 00	0.18998E-05	0.34328E-05	0.50078E-05	0.61536E-05	0.68452E-05	0.72247E-05	0.74234E-05	0.75254E-05	0.75771E-05	0.76029E-05	0.76159E-05	0.56696E-05	0.76259E-05	0.76275E-05	0.76284E-05	0.76287E-05	0.76290E-05	0.76292E-05	0.76290E-05
ROW 2	0.	1.00000E 00	0.36697E-06	0.18578E-05	0.38621E-05	0.54621E-05	0.64654E-05	0.70256E-05	0.73215E-05	0.74736E-05	0.75511E-05	0.75897E-05	0.76095E-05	0.76194E-05	0.76244E-05	0.76266E-05	0.76281E-05	0.76285E-05	0.76287E-05	0.76295E-05
ROW 3	0.	0.	1.00000E 00	0.73395E-06	0.37157E-05	0.77241E-05	0.10924E-04	0.12931E-04	0.14051E-04	0.14643E-04	0.14947E-04	0.15102E-04	0.15180E-04	0.15219E-04	0.15239E-04	0.15249E-04	0.15253E-04	0.15256E-04	0.15257E-04	0.15257E-04
ROW 4	0.	0.	0.	0.99999E 00	0.14679E-05	0.74314E-05	0.15448E-04	0.21848E-04	0.25862E-04	0.28102E-04	0.29286E-04	0.29894E-04	0.30205E-04	0.30359E-04	0.30437E-04	0.30477E-04	0.30497E-04	0.30506E-04	0.30512E-04	0.30514E-04
ROW 5	0.	0.	0.	0.	0.99998E 00	0.29358E-05	0.14863E-04	0.30896E-04	0.43696E-04	0.51723E-04	0.56205E-04	0.58572E-04	0.59790E-04	0.60409E-04	0.60719E-04	0.60875E-04	0.60955E-04	0.60995E-04	0.61012E-04	0.61025E-04
ROW 6	0.	0.	0.	0.	0.	0.99997E 00	0.58716E-05	0.29725E-04	0.61792E-04	0.87392E-04	0.10345E-03	0.11241E-03	0.11715E-03	0.11958E-03	0.12082E-03	0.12144E-03	0.12175E-03	0.12191E-03	0.12199E-03	0.12202E-03
ROW 7	0.	0.	0.	0.	0.	0.	0.99994E 00	0.11744E-04	0.59451E-04	0.12358E-03	0.17478E-03	0.20689E-03	0.22482E-03	0.23429E-03	0.23916E-03	0.24163E-03	0.24287E-03	0.24350E-03	0.24382E-03	0.24398E-03
ROW 8	0.	0.	0.	0.	0.	0.	0.	0.99988E 00	0.23488E-04	0.11890E-03	0.24717E-03	0.34957E-03	0.41379E-03	0.44964E-03	0.46858E-03	0.47831E-03	0.48327E-03	0.48575E-03	0.48700E-03	0.48764E-03
ROW 9	0.	0.	0.	0.	0.	0.	0.	0.99976E 00	0.46976E-04	0.23780E-03	0.49433E-03	0.69915E-03	0.82758E-03	0.89928E-03	0.93716E-03	0.95662E-03	0.96654E-03	0.97150E-03	0.97400E-03	0.97400E-03
ROW 10	0.	0.	0.	0.	0.	0.	0.	0.	0.99951E 00	0.93952E-04	0.47560E-03	0.98868E-03	0.13983E-02	0.16552E-02	0.17986E-02	0.17986E-02	0.18743E-02	0.19132E-02	0.19331E-02	0.19430E-02
ROW 11	0.	0.	0.	0.	0.	0.	0.	0.	0.	0.99903E 00	0.18790E-03	0.95122E-03	0.19773E-02	0.27966E-02	0.33103E-02	0.35971E-02	0.37486E-02	0.38265E-02	0.38661E-02	0.38661E-02
ROW 12	0.	0.	0.	0.	0.	0.	0.	0.	0.	0.	0.	0.	0.99805E 00	0.37581E-03	0.19024E-02	0.39547E-02	0.55931E-02	0.66206E-02	0.74972E-02	0.76530E-02
ROW 13	0.	0.	0.	0.	0.	0.	0.	0.	0.	0.	0.	0.	0.	0.99611E 00	0.75162E-03	0.38048E-02	0.79094E-02	0.11186E-01	0.13241E-01	0.14388E-01
ROW 14	0.	0.	0.	0.	0.	0.	0.	0.	0.	0.	0.	0.	0.	0.	0.99222E 00	0.15032E-02	0.76097E-02	0.15819E-01	0.22372E-01	0.26482E-01
ROW 15	0.	0.	0.	0.	0.	0.	0.	0.	0.	0.	0.	0.	0.	0.	0.	0.98444E 00	0.30065E-02	0.15219E-01	0.31637E-01	0.44745E-01
ROW 16	0.	0.	0.	0.	0.	0.	0.	0.	0.	0.	0.	0.	0.	0.	0.	0.	0.96887E 00	0.60129E-02	0.30439E-01	0.63275E-01
ROW 17	0.	0.	0.	0.	0.	0.	0.	0.	0.	0.	0.	0.	0.	0.	0.	0.	0.	0.93774E 00	0.12026E-01	0.60877E-01
ROW 18	0.	0.	0.	0.	0.	0.	0.	0.	0.	0.	0.	0.	0.	0.	0.	0.	0.	0.	0.87549E 00	0.24052E-01
ROW 19	0.	0.	0.	0.	0.	0.	0.	0.	0.	0.	0.	0.	0.	0.	0.	0.	0.	0.	0.75098E 00	0.48103E-01
ROW 20	0.	0.	0.	0.	0.	0.	0.	0.	0.	0.	0.	0.	0.	0.	0.	0.	0.	0.	0.	0.50195E 00

FIG. A-6 MARKOV MATRIX

means all material in the size range  $\frac{X_0}{4}$  to  $\frac{X_0}{2}$ . For the coefficient  $a_{mm}$  is put the fraction material in size range  $m$  will remain in that size range after a time  $\Delta t$ . For the coefficient  $a_{m-1m}$  is put the fraction of material which broke from size range  $m$  to size range  $m-1$  in time  $\Delta t$ . For the coefficient  $a_{m-2,m}$  is put the fraction of material which broke from size  $m$  to size range  $m-2$  in time  $\Delta t$ . In other words, column  $m$  is a weight retained screen analysis of the material after time  $\Delta t$  if all the material were initially in size range  $m$ . The screens are a geometric series with a ratio of two between screen openings. Column 2 is very similar to column 1 except it is a weight retained screen analysis of all material which initially was in size range  $m-1$ . Consequently,  $a_{mm-1}$  is zero, for no material can break from size  $m-1$  to size  $m$ . Column  $m-2$  is a screen analysis of all material which initially started from size range  $m-2$ . Thus  $a_{mm-2} = a_{m-1, m-2} = 0$ . The other columns are made up the same way. The sum of the coefficients in each column is one because the material which started in a given size range must end up in a some size range if the mass is to be conserved. Consequently, all coefficients in row 1 represent the cumulative weight finer material below size range 2, ( $m-19$ ).

If the initial Markov matrix,  $[V]$ , is post multiplied by a screen analysis of the feed, a column matrix,  $[F]$ , the result is a screen analysis of the product, a column matrix,  $\Theta$ , after one time interval,  $\Delta t$ .

$$[V] \cdot [F] = [\Theta] \quad (125)$$

Now  $[\Theta]$  can be considered the feed for the grinding during the second

$\Delta t$ . Thus:

$$[V] \cdot [\theta] = [\theta_2] \quad (126)$$

Substituting equation 125 in 126

$$[V] \cdot [V] \cdot [F] = [\theta_2] \quad (127)$$

Carrying out the matrix multiplication

$$[V]^2 \cdot [F] = [\theta_2] \quad (128)$$

In other words, if the column matrix  $[F]$  is premultiplied by the square of the initial Markov matrix then the result is the product matrix,  $[\theta_2]$ , after 2 intervals of time,  $\Delta t$ . In a like manner, the product after 4 time intervals,  $[\theta_4]$ , is obtained from the following equation:

$$[V]^4 \cdot [F] = [\theta_4] \quad (129)$$

After 8 time intervals:

$$[V]^8 \cdot [F] = [\theta_8] \quad (130)$$

In equation 124 there are two arbitrary parameters and one arbitrary function. The arbitrary parameters are  $r$ , the size ratio, which influences the shape of the screen analysis and  $X_0$ , which is the largest initial particle. The arbitrary function,  $P(x)$ , expresses the way the probability of a particle breaking varies with size for a fixed time,  $\Delta t$ .

$X_0$  is the largest size particle and all other particles size,  $x$ ,

are expressed as the ratio,  $x/X_0$ . Essentially, this means that column 20 in the matrix initially contains particles of size  $X_0/2$  to  $X_0$ ; column 19,  $X_0/4$  to  $X_0/2$ ; column 18,  $X_0/8$  to  $X_0/4$  etc.

The size ratio,  $r$ , determines what fraction of the mass will fall in a given size fraction if equation 35 is used to express the mass frequency distribution. Four different size ratios were used:  $r = 2, 4, 8, 16$  and so designated. To test the effect of another mass frequency distribution, a Gaudin-Schuhmann equation, was used. It is:

$$M(x) = \frac{4dx}{X_0} \quad 0 \leq x \leq \frac{X_0}{4} \quad (131)$$

When equation 131 was used the matrix was entitled  $R = 4, S = 1$ .

The arbitrary function  $P(x)$  designates how the probability of a particle breaking varies with size. Five different functions were used. In each case the function was constructed so that 50% of the particles most likely to be broken would be broken. The functions were:

$$P(x) = 0.5 \quad 0 \leq x \leq X_0 \quad (132)$$

$$P(x) = 0.5 \left(\frac{x}{X_0}\right)^{1/2} \quad 0 \leq x \leq X_0 \quad (133)$$

$$P(x) = 0.5 \left(\frac{x}{X_0}\right)^1 \quad 0 \leq x \leq X_0 \quad (134)$$

$$P(x) = 0.5 \left(\frac{x}{X_0}\right)^2 \quad 0 \leq x \leq X_0 \quad (135)$$

$$P(x) = \begin{cases} 0.5 \left(16 \frac{x}{X_0}\right) & 0 \leq x \leq \frac{X_0}{16} \\ -0.5 \left(\frac{x}{X_0}\right) + \frac{17}{32} & \frac{X_0}{16} \leq x \leq X_0 \end{cases} \quad (136)$$

The  $P(x)$  function in equation 136 was designated as  $P(x) = \text{comp. 1.}$

All the others were expressed as:

$$P = 0.5 E_0; \quad 0.5 E_{1/2}; \quad 0.5 E_1; \quad 0.5 E_2$$

where  $E_0$  means  $\left(\frac{x}{x_0}\right)^0$ ;  $E_1$  means  $\left(\frac{x}{x_0}\right)^1$  etc.

The matrices are designated in the following manner MARKOV  $t = 32$ ,  $P = 0.5 E_{1/2}$ ,  $R = 8$ . This means that it is the initial Markov matrix raised to the 32nd power (i.e. when 32  $\Delta t$ 's had elapsed). The arbitrary probability of breakage function is:

$$P(x) = 0.5 \left(\frac{x}{x_0}\right)^{1/2} \quad (137)$$

and the reduction ratio is equal to eight.

The Markov matrices alternate with the output matrices. The output matrices are the product of the preceding Markov matrix with the 20 by 20 feed matrix. The feed matrix consists of screen analysis of 20 possible feeds. The output matrix consists of the predicted screen analysis of 20 products for the 20 given feeds. Thus column 1 of the matrix designated OUTPUT  $t = 32$ ,  $P = 0.5 E_{1/2}$ ,  $R = 8$  is the pre-multiplication of the corresponding Markov matrix with column 1 of the feed matrix. In other words, column 1 of the output matrix is the predicted screen analysis of the feed in column 1 of the feed matrix for 32  $\Delta t$ 's plus the other conditions.

Since the squaring of a 20 by 20 matrix using a hand computer takes about one week it was not possible to do the work by hand. Instead the

calculations were performed on the IBM 709 computer. A general purpose matrix abstraction program, called 9MA, was used.

The program may be obtained from Share. The instruction to the computer and the data appear in the appendix. Also both the Markov and Output matrices are tabulated in the appendix.



## RESULTS

The results are divided into three parts. The first is the derived equation for the mass frequency distribution; a comparison of the derived equation with other experimental and theoretical plots is given in figures 1-3. The second part is the analytical solution to equation 77, the integral differential equation. The solution is derived in a previous section and the results for a given set of boundary conditions are plotted in figure 16. The third part is the numerical solution to equation 77 with different boundary conditions. The tabulated results of the calculations appear in the appendix. Selected results have been graphed in figures 6-15 and figures 17-29. These results may be compared with the analytical solution in figure 16 and the experimental results in figures 4, 5, 30, 31, 32 and 33.

The mass frequency distribution, MFD, of the fragments of a particle broken once is derived in the section on Single Fracture. In the integrated form, this MFD expresses the weight of material finer than a given size  $x$ . Equation 47 is:

$$\frac{W(x)}{W_0} = 1 - \left(1 - \frac{x}{X_0}\right)^r \quad (138)$$

in which  $W(x)$  is weight of material finer than size  $x$ .  $W_0$  is the total weight of the initial particle,  $X_0$  is the characteristic dimension of the initial particle and  $r$  is the size ratio. Figure 1 is a comparison of three curves which represent CWF, cumulative weight finer, of a particle broken once. One curve is a plot of equation 138 with  $W_0 = 1$ ,

$X_0 = 1$  and  $r = 2$ . The second curve is a Gaudin-Schuhmann equation and is:

$$\frac{W(x)}{W_0} = \left(\frac{rx}{X_0}\right)^m \quad (139)$$

where  $W_0$ ,  $X_0$  and  $r$  have the same values as before. The slope,  $m$ , is set at 1 to conform to the other two equations and the experimental results of Hukki<sup>(5)</sup>. The third equation is the one derived by Gilvarry<sup>(13)</sup> and is:

$$\frac{W(x)}{W_0} = 1 - e^{-\frac{rx}{X_0}} \quad (140)$$

where  $W_0$ ,  $X_0$  and  $r$  are as before. In the smaller size ranges, all three equations approach one another asymptotically and have a slope of 1. The derived equations bend to the right of the Gaudin-Schuhmann equation. At  $x = X_0$  the Gilvarry equation states that the amount of material equal to, or finer than, the original particle size is 86.5% of the original mass. This equation does not conserve mass, whereas the derived equation does.

In figure 2 experimental data from Hukki's<sup>(5)</sup> thesis is compared with equation 140. Galena, the material being crushed, was chosen because the initial particle size could be calculated from the initial weights by assuming the particle to be a cube. The experimental results and the derived equation closely agree. The full plot of Hukki's<sup>(5)</sup> data on galena is shown in figure 3. A comparison of figures 1 and 2 show that the other two CWF curves would not fit the data as well.

An analytical solution to equation 77 has been put in the same form (in equation 113) as the numerical solutions. Equation 113 has been plotted

for 8 values of  $\Delta t$  in figure 16. Figures 17-21 are numerical solutions of equation 77 and differ from figure 16 only in the value of the reduction ratio. Thus, figures 16-21 are a complete family of figures. It is interesting to note the similarity of form. All the curves have the same shape, spacing, maximum and evenness of plot. The numerical and analytical solutions appear compatible. The slope of the curves approaches 1 in the lower size ranges.

The third part of the results is the tabulation and plotting of the numerical solutions of equation 77. The appendix contains the tabulation of the solutions, and figures 6-29 are plots of the numerical solution for the same boundary condition. The analytical solution in figure 16 also has the same boundary condition. The boundary condition was chosen such that all of the material was initially at size  $X_0$ .

There are five sets of figures: 6-10, 11-15, 16-21, 22-25 and 26-29. The first set of figures (6-10) represents solutions to equation 77 where the probability of a particle being broken in a given length of time is independent of size. The second set of figures (11-15) gives solutions to equation 77 where the probability of a particle being broken is proportional to the square root of the particle size. As shown in the section on Single Fracture, this is the condition that would be expected in a rod mill. One of the plotted curves in figure 11 is taken from figure 4.

In the third set of figures (16-21) solutions are given to equation 77 where the probability of a particle being broken is proportional to the first power of the particle size. The fourth set of figures (22-25) gives solutions to equation 77 where the probability of a particle being broken

is proportional to the square of the particle size. The fifth set of figures (26-29) is a composite of two probability functions. The probability of a particle being broken rises linearly until the  $\frac{x}{x_0}$  ratio is 1/16 and then falls linearly. This may be the condition in a ball mill where some particles are so large that they are not likely to be broken. For example, in a ball mill the angle of nip may be exceeded by the larger particle and thus greatly reduce their chance of being broken.

Within each of the five groups there is a variation in the size ratio, and a figure where the value of  $r$  is equal to 2, 4, 8 and 16. The mass frequency distribution used with these four values is the one derived in the section on Single Fracture, equation 35.

To test the effect of another mass frequency distribution, a Gaudin-Schuhmann <sup>(6)</sup> equation with a slope of 1 and a size ratio of 4 was used. The figures using this mass frequency distribution are figures 8, 13 and 19, while figure 16 has a size ratio of one. The curves in this figure 16 come from the analytical solution of equation 77. They are included in group 3 because they resemble the numerical solution so closely.

Figures 4, 5, 30, 31, 32 and 33 are taken from Gaudin <sup>(4)</sup> as examples of experimental work.

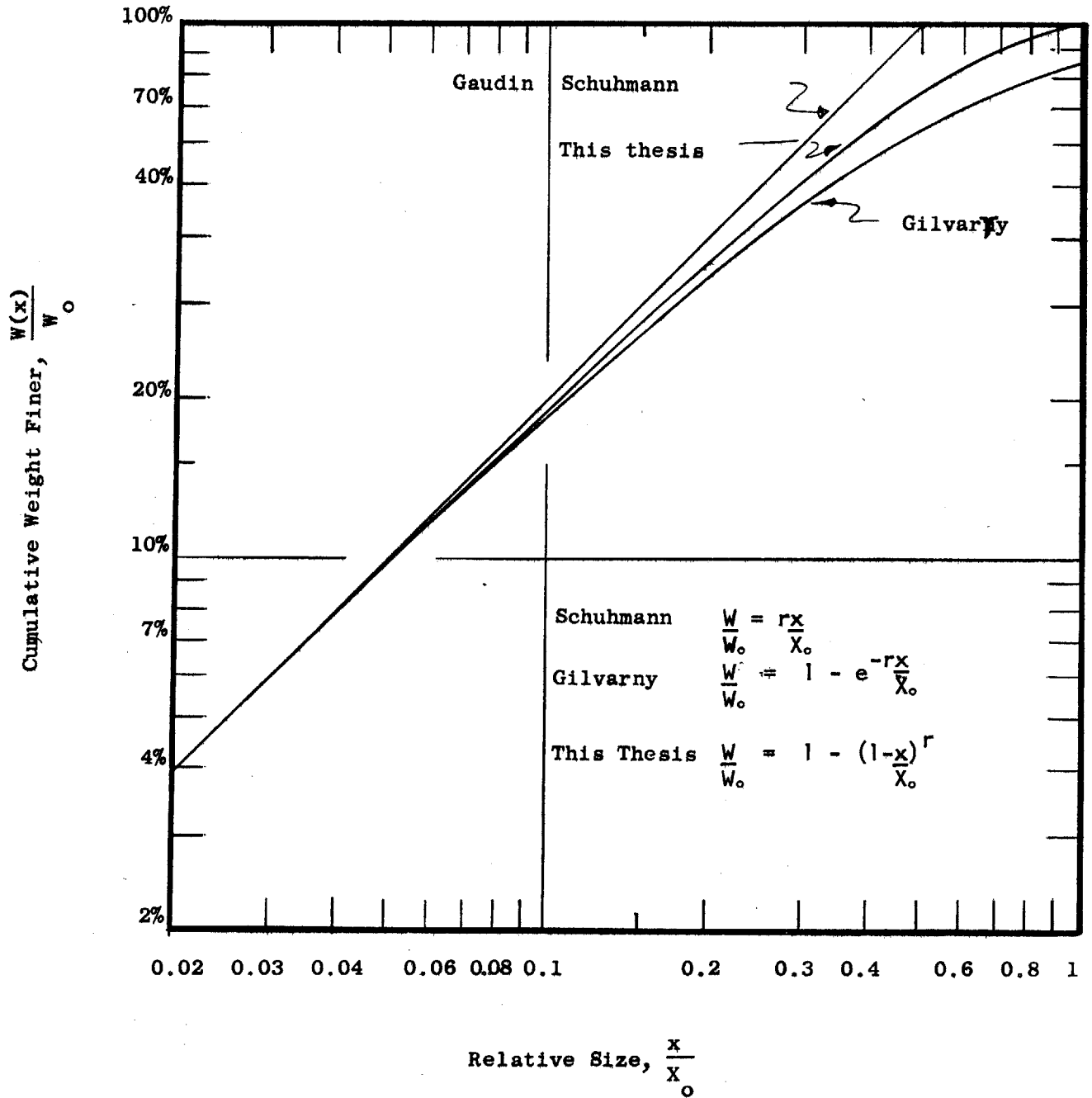


Fig. 1 -- Comparison of the three major equations used to describe the cumulative weight finer of the fragments obtained by single fracture. The reduction ratio is 2.0.

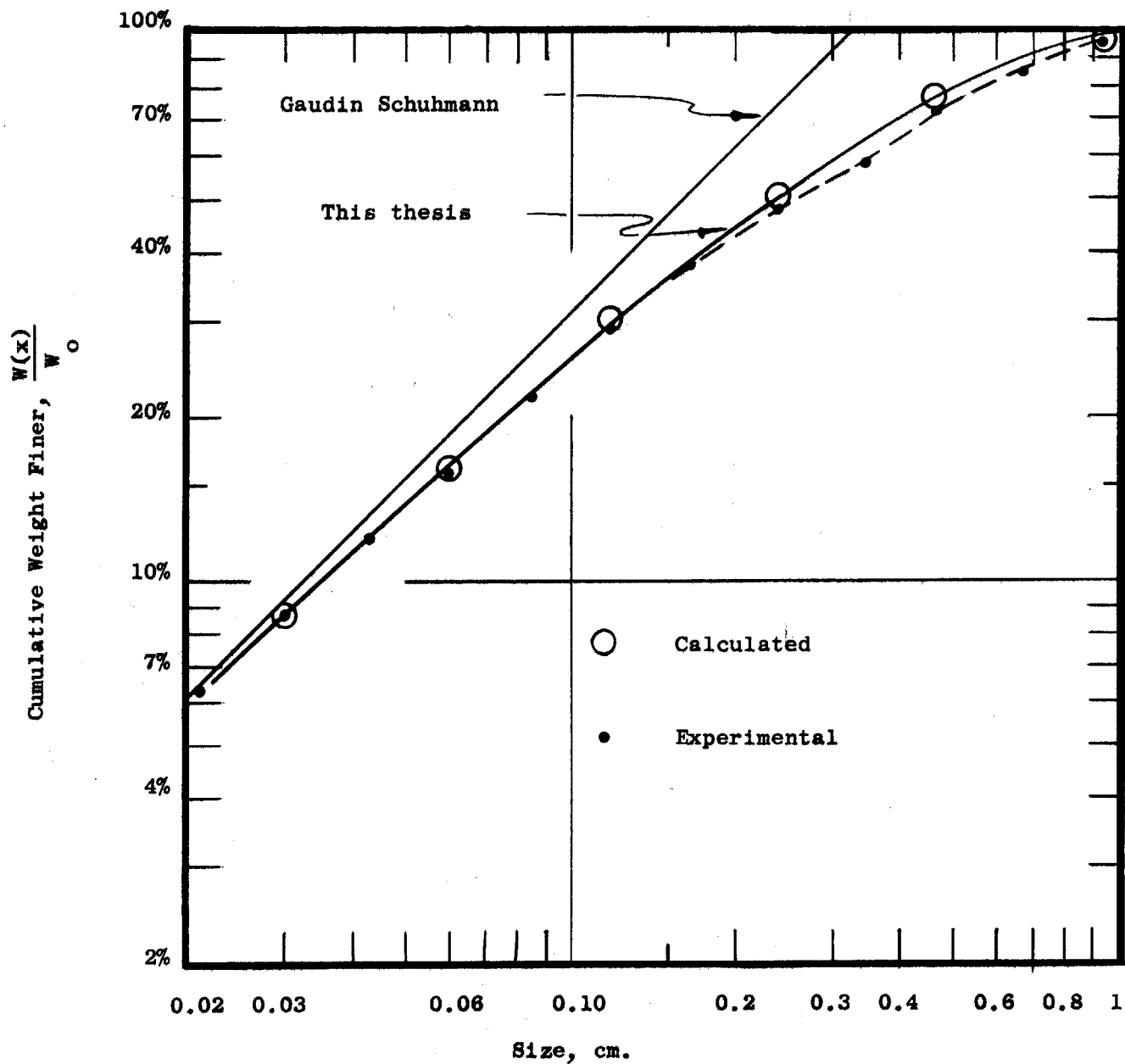


Fig. 2 -- Comparison of Hukki's experimental data for galena crushed in a single-blow pendulum crusher with the Equation derived in this thesis for single fracture. Dots represent Hukki's points and circles theoretical points.

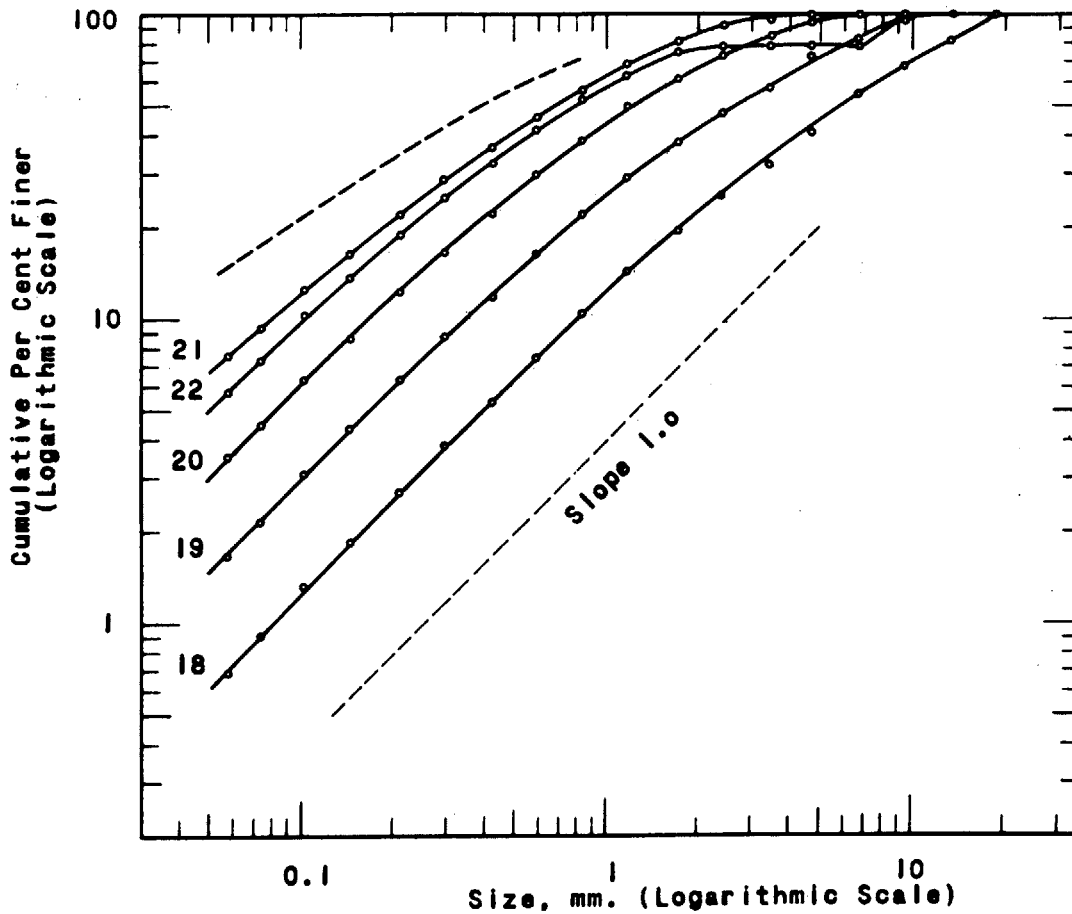


FIG. 3 - Experimental log-log size distribution plots of galena broken during single fracture. After Hukki(5).

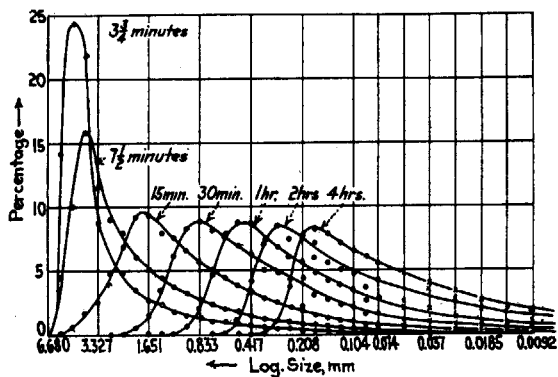


FIG. 4 - Experimental semi-log size distribution plots of quartz ground in a rod mill for different lengths of time. After Gaudin(4).

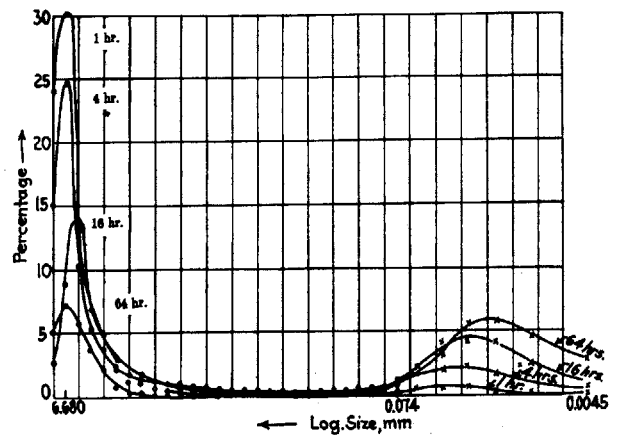


FIG. 5 - Experimental semi-log size distribution plots of quartz ground in a ball mill for different lengths of time. After Gaudin(4).

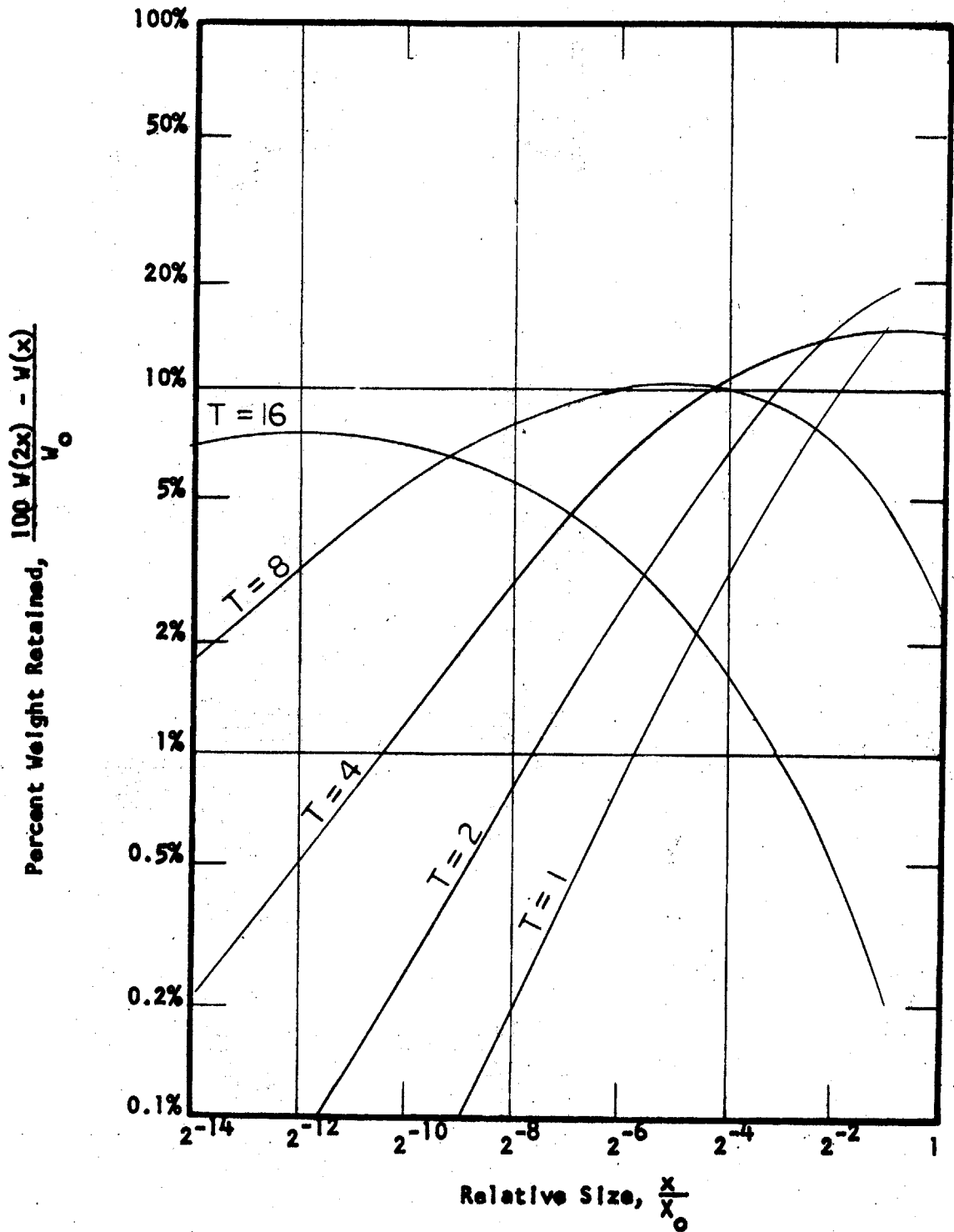


Fig. 6 -- Calculated plots of log percent weight retained vs. log size for different time intervals.  $P(x) = 1/2$ ;  $r = 2$ .



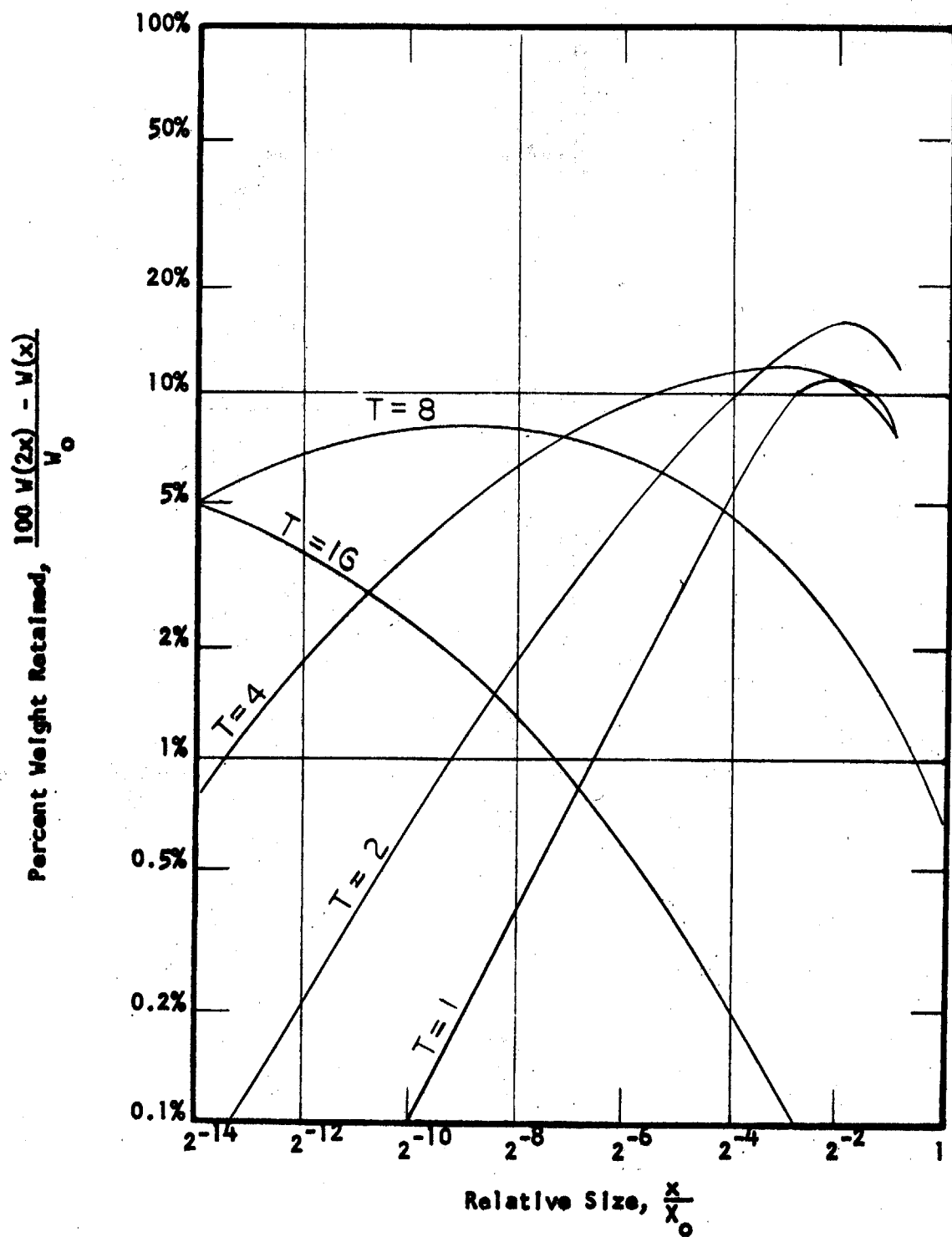


Fig. 7 -- Calculated plots of log percent weight retained vs. log size for different time intervals.  $P(x) = 1/2$ ;  $r = 4$ .

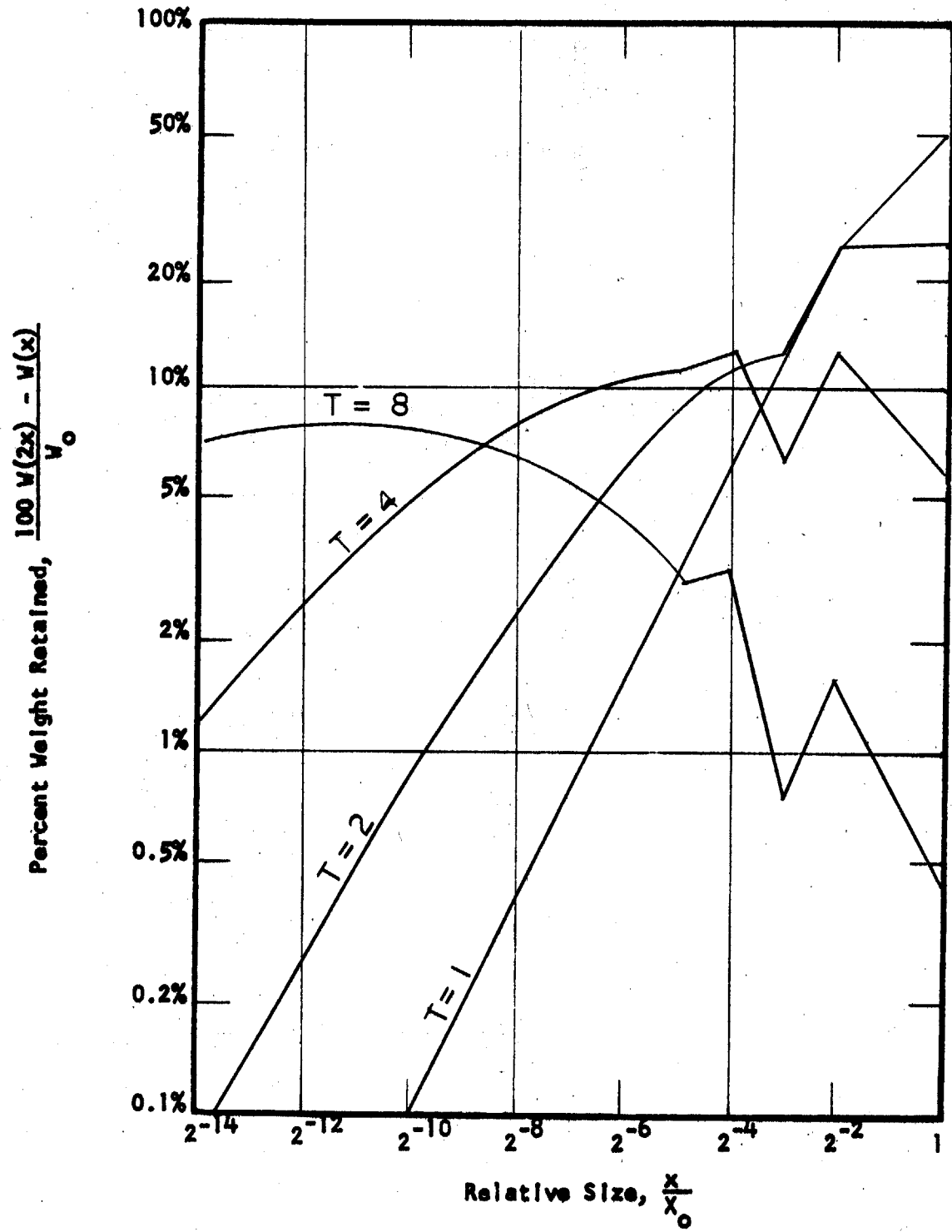


Fig. 8 Calculated plots of log percent weight retained vs. log size for different time intervals.  $P(x) = 1/2$ ;  $r = 4$   $s = 1$  (Gaudin-Schuhmann equation used).

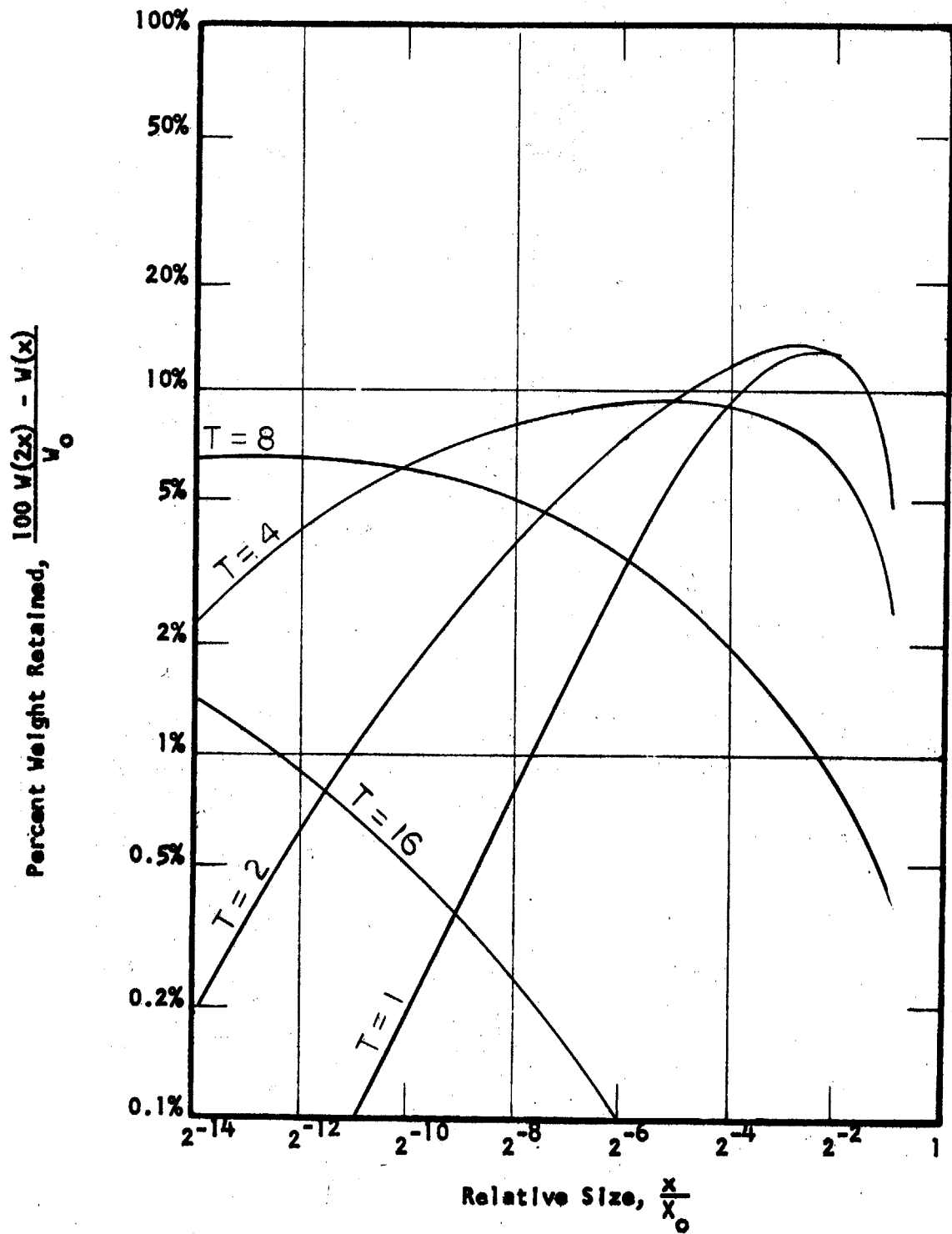


Fig. 9 Calculated plots of log percent weight retained vs. log size for different time intervals.  $P(x) = 1/2$ ;  $r = 8$ .

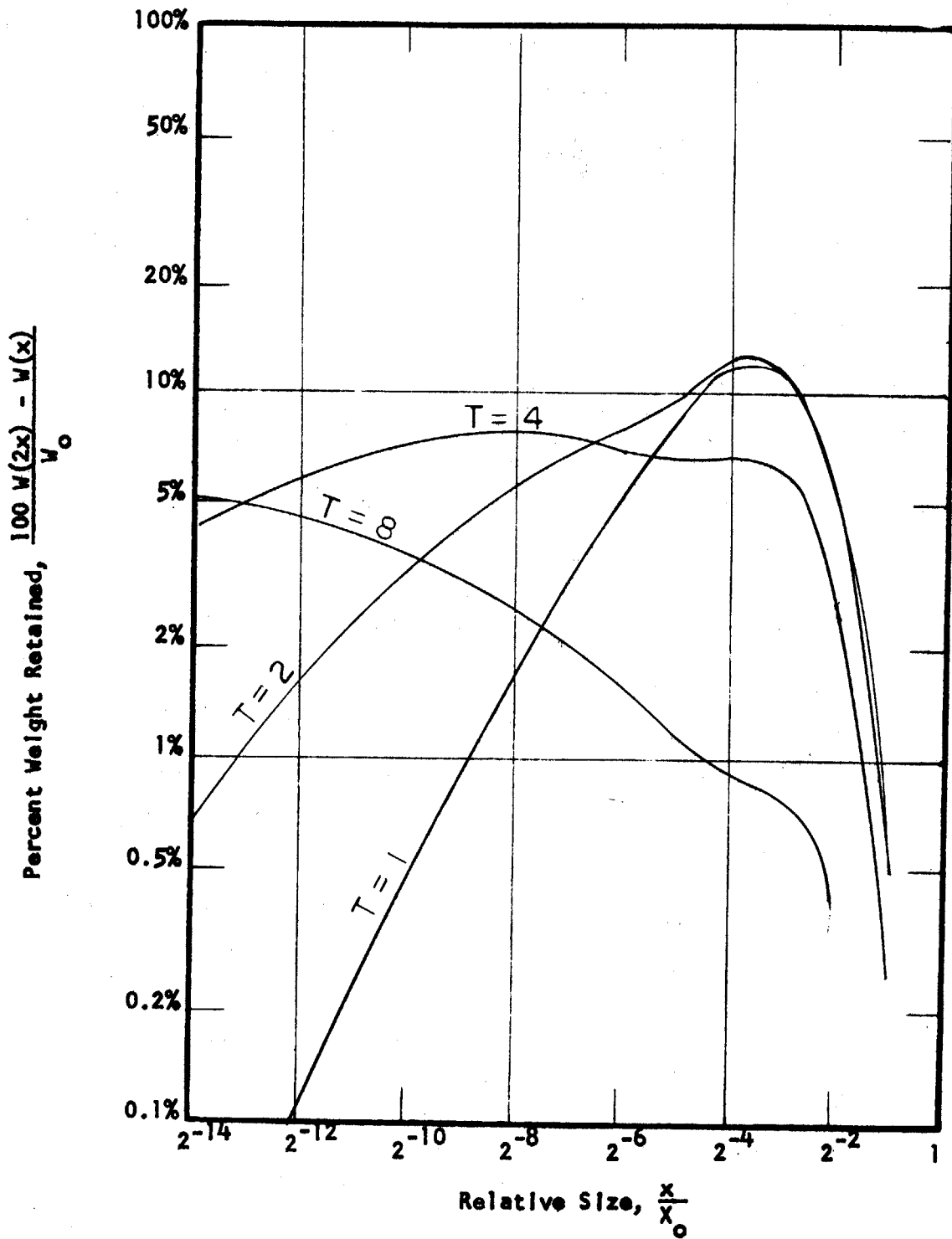


Fig. 10 --Calculated plots of log percent weight retained vs. log size for different time intervals.  $P(x) = 1/2$ ;  $r = 16$ .

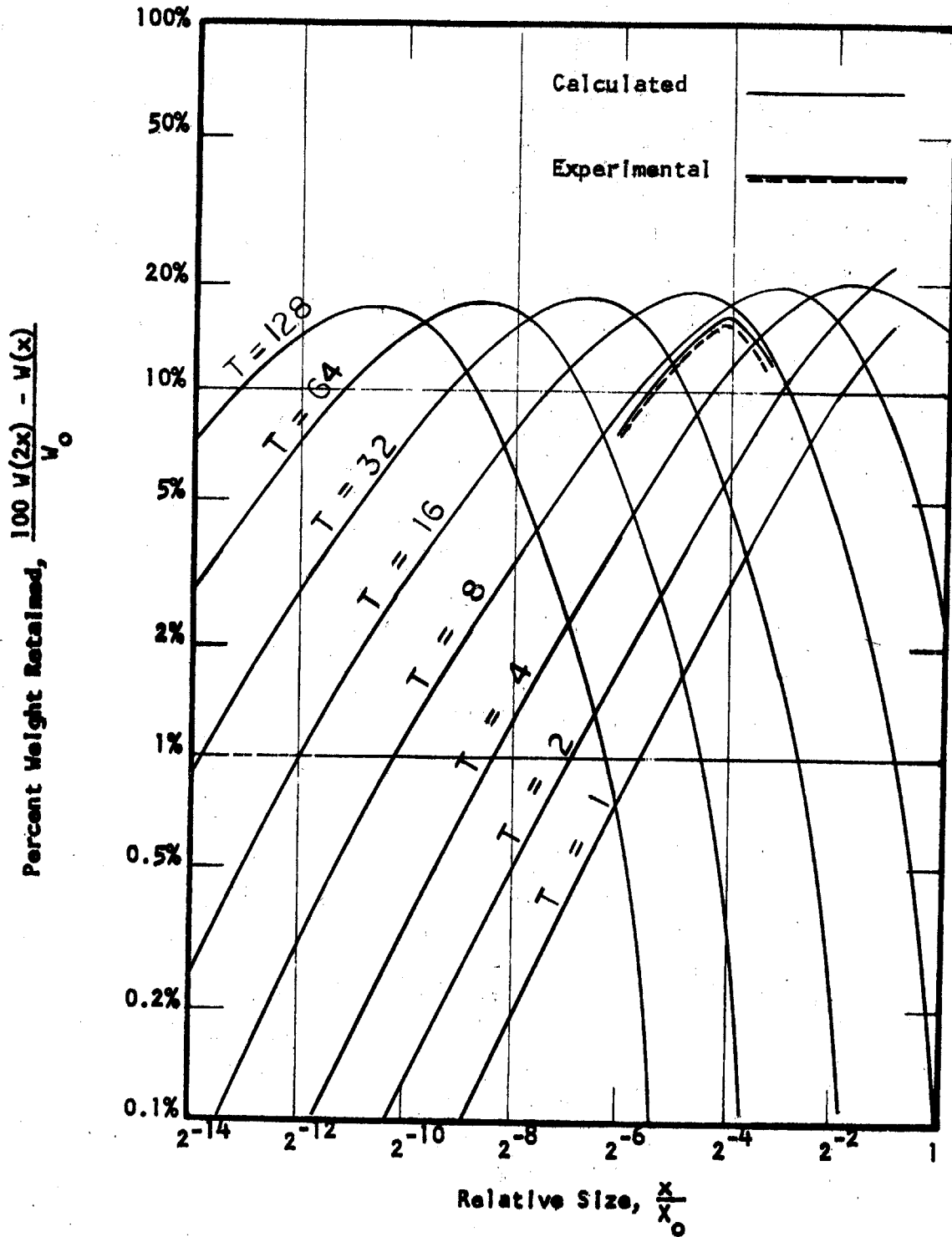


Fig. 11 -- Calculated plots of log percent weight retained vs. log size for different time intervals.  $P(x) = 1/2x^{1/2}$ ;  $r = 2$ . Note replot of experimental data taken from Figure 4.

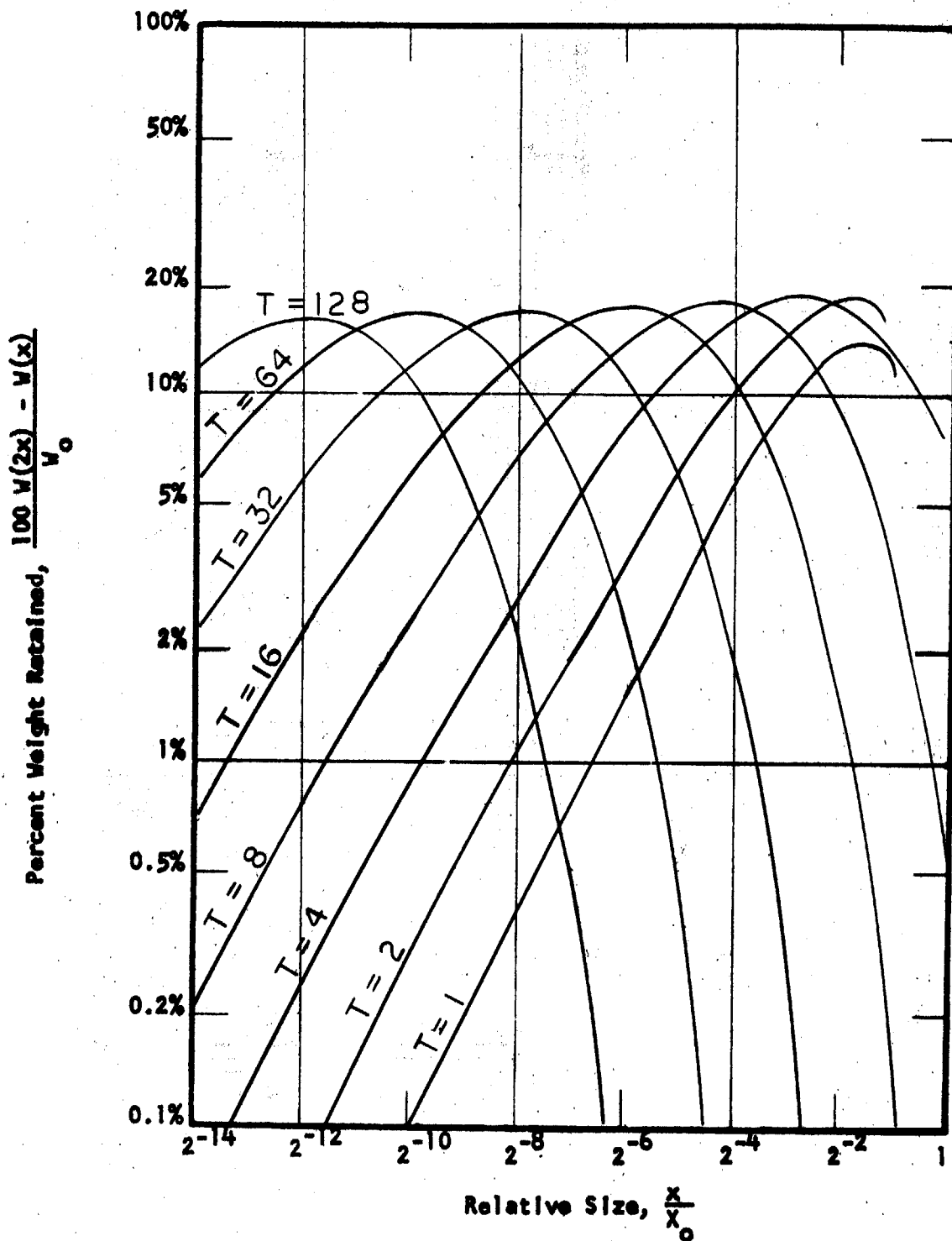


Fig. 12 -- Calculated plots of log percent weight retained vs. log size for different time intervals.  $P(x) = 1/2x^{1/2}$ ;  $r = 4$ .

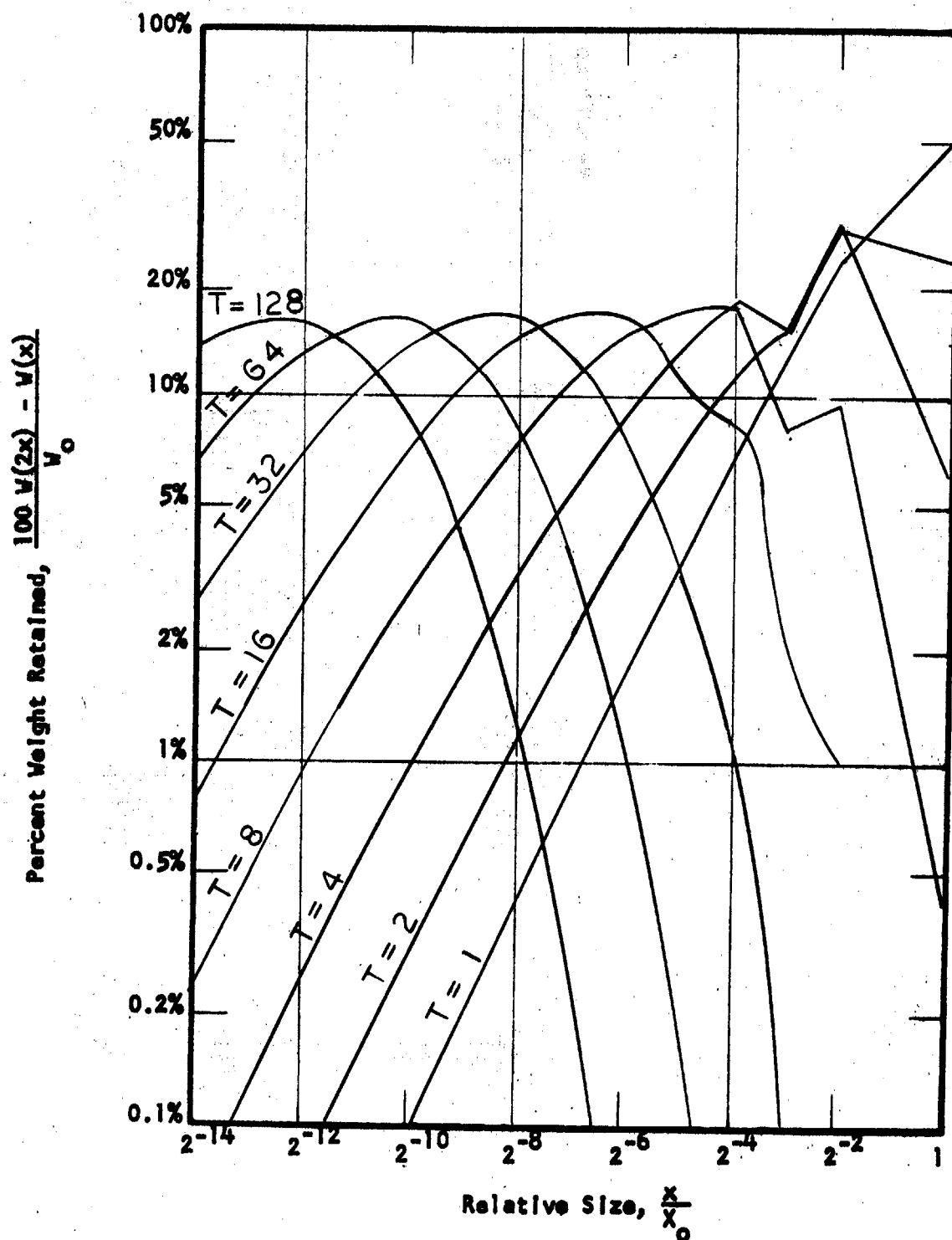


Fig. 13 -- Calculated plots of log percent weight retained vs. log size for different time intervals.  $P(x) = 1/2x^{1/2}$ ;  $r = 4$ ,  $s = 1$  (Gaudin-Schumann equation used).

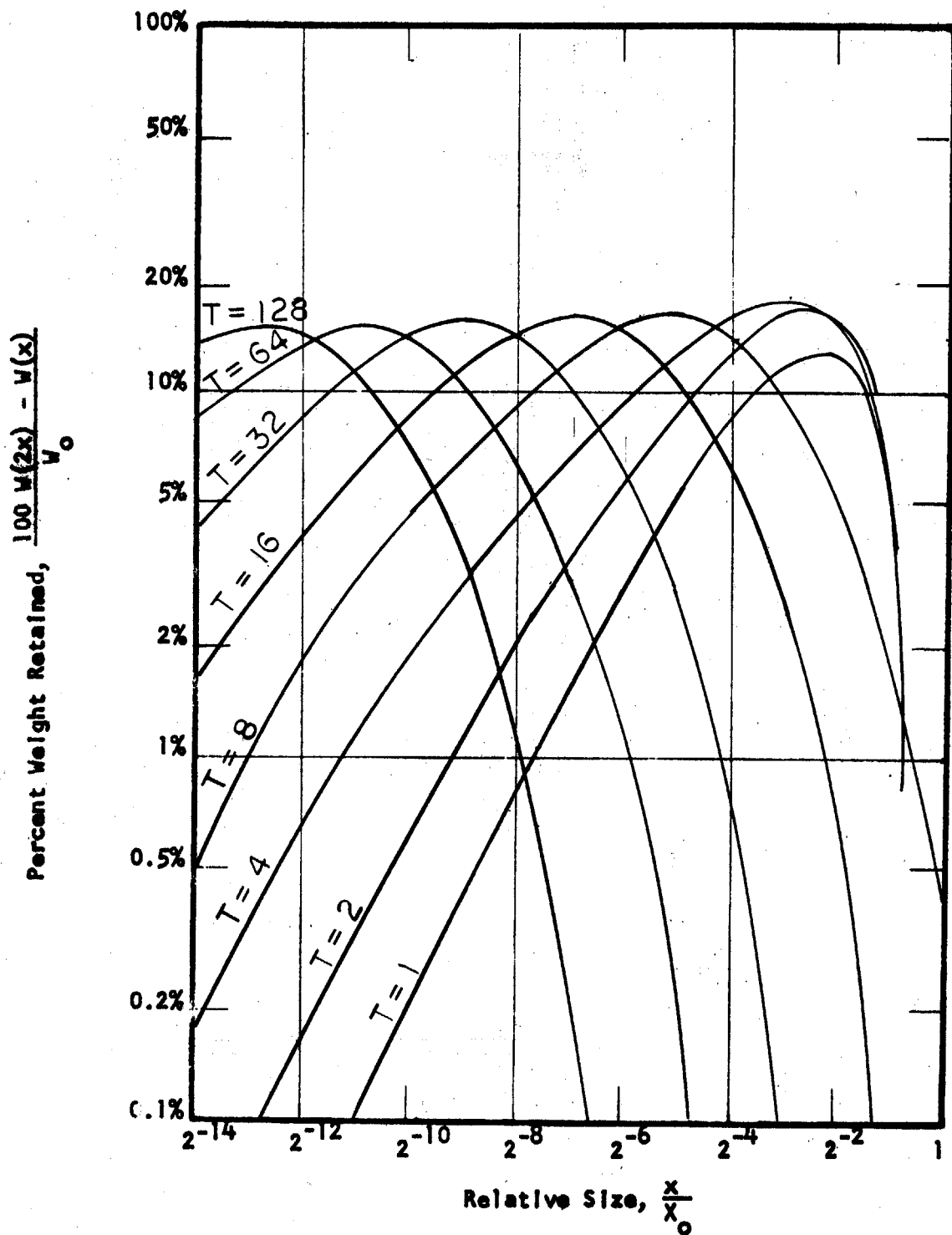


Fig. 14 -- Calculated plots of log percent weight retained vs. log size for different time intervals.  $P(x) = 1/2x^{1/2}$ ;  $r = 8$ .



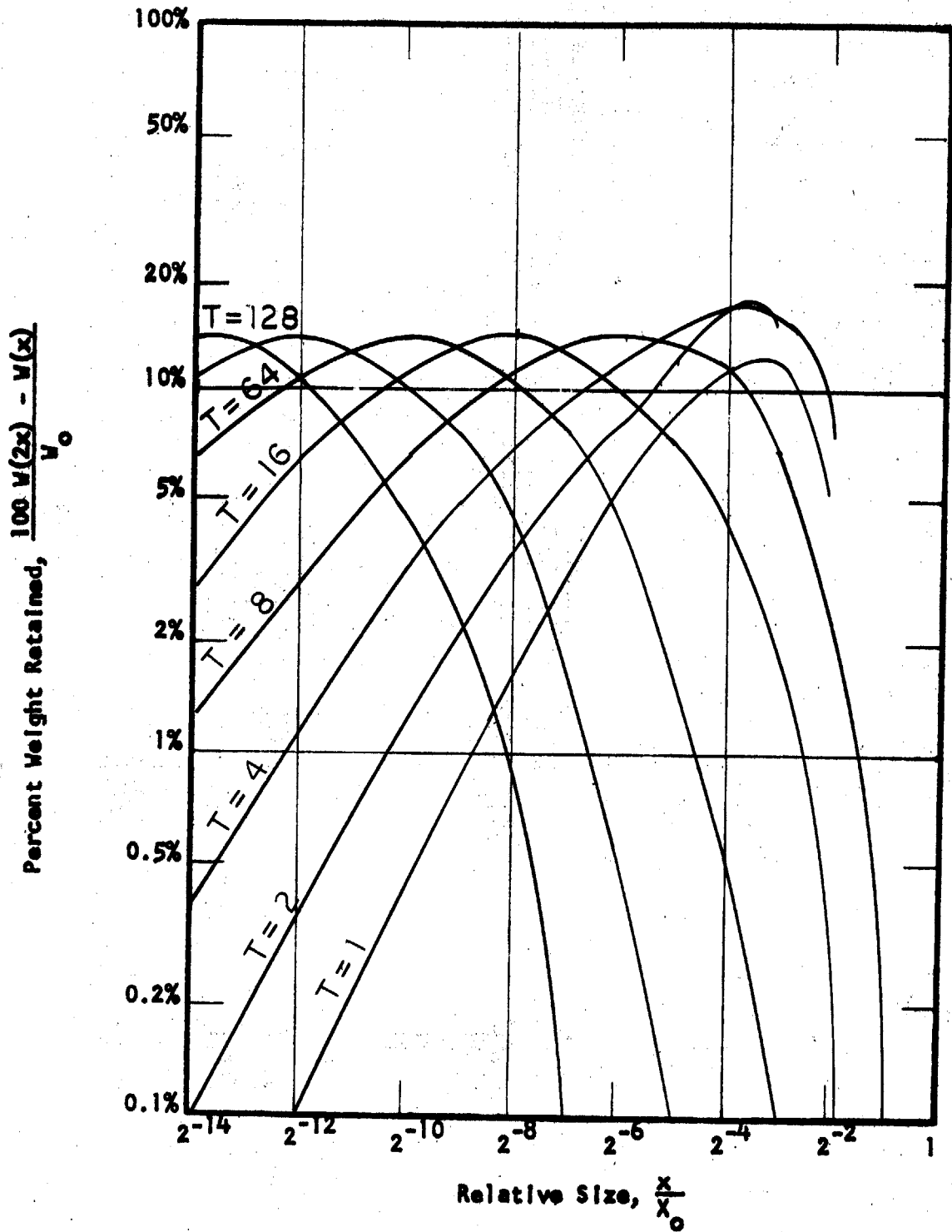


Fig. 15 -- Calculated plots of log percent weight retained vs. log size for different time intervals.  $P(x) = 1/2x^{1/2}$ ;  $r = 16$ .

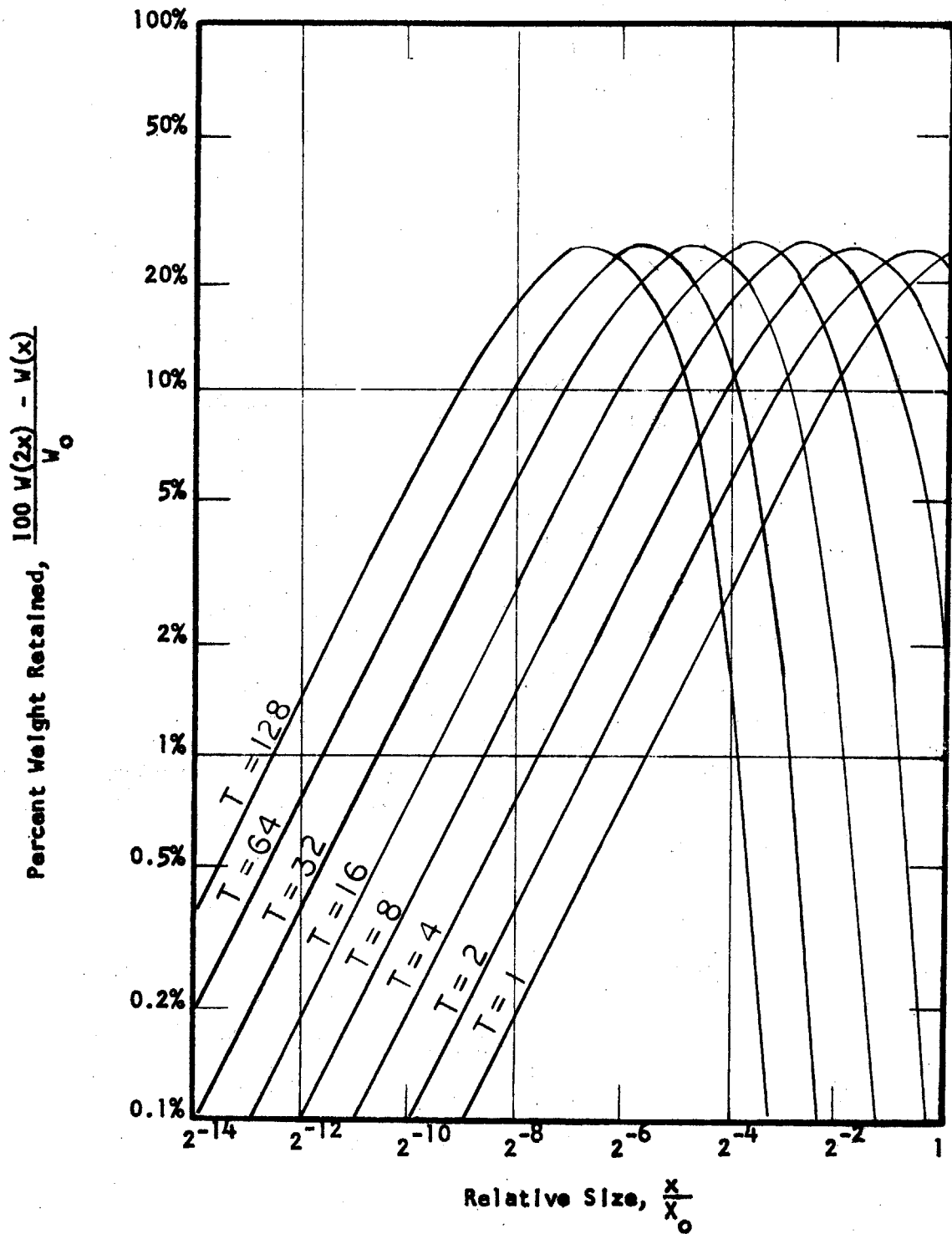


Fig. 16 - Theoretical plots of log percent weight retained vs. log size for different time intervals.  $P(x) = 1/2x$ ;  $r = 1$ .

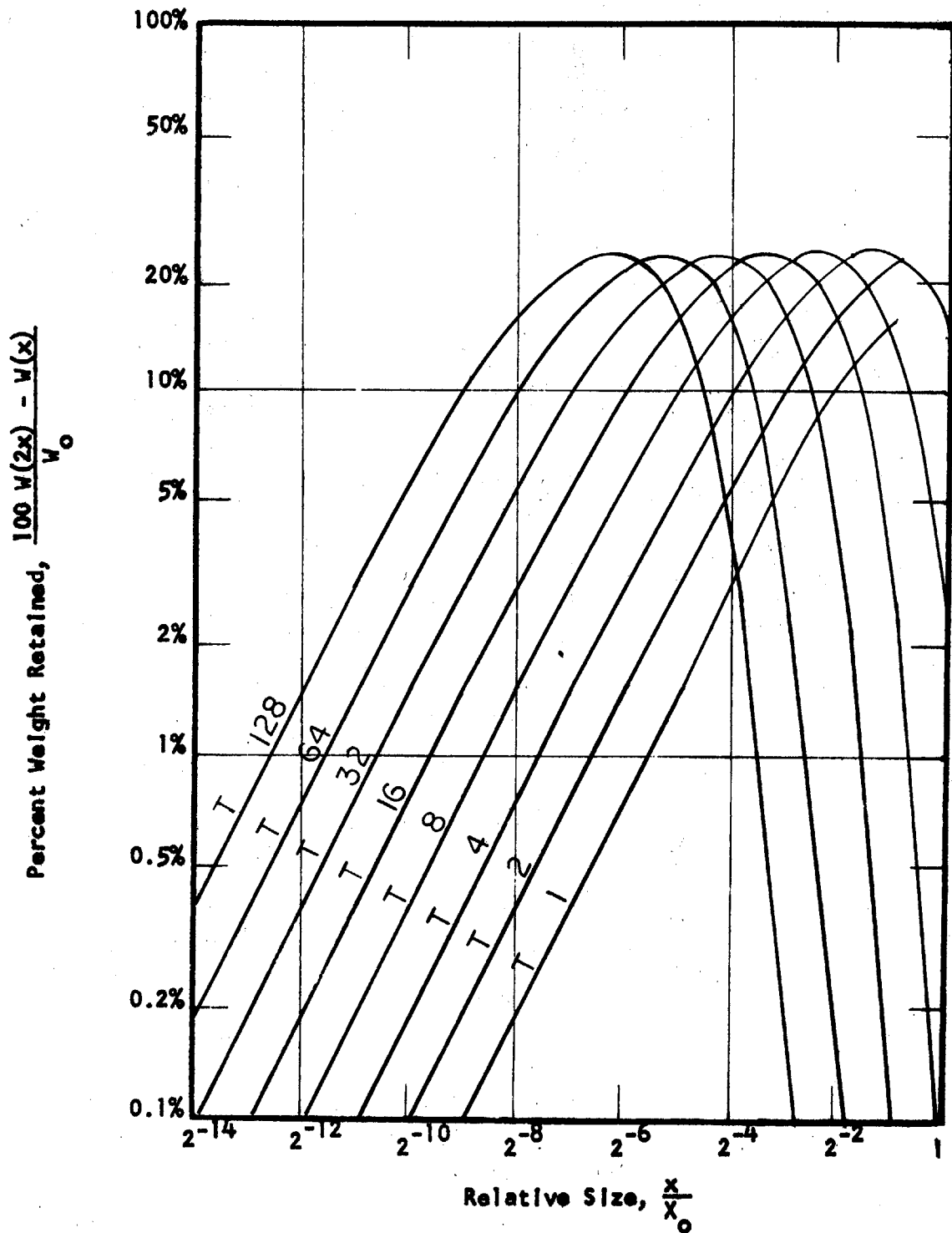


Fig. 17 -- Calculated plots of log percent weight retained vs. log size for different time intervals.  $P(x) = 1/2x$  ;  $r = 2$ .

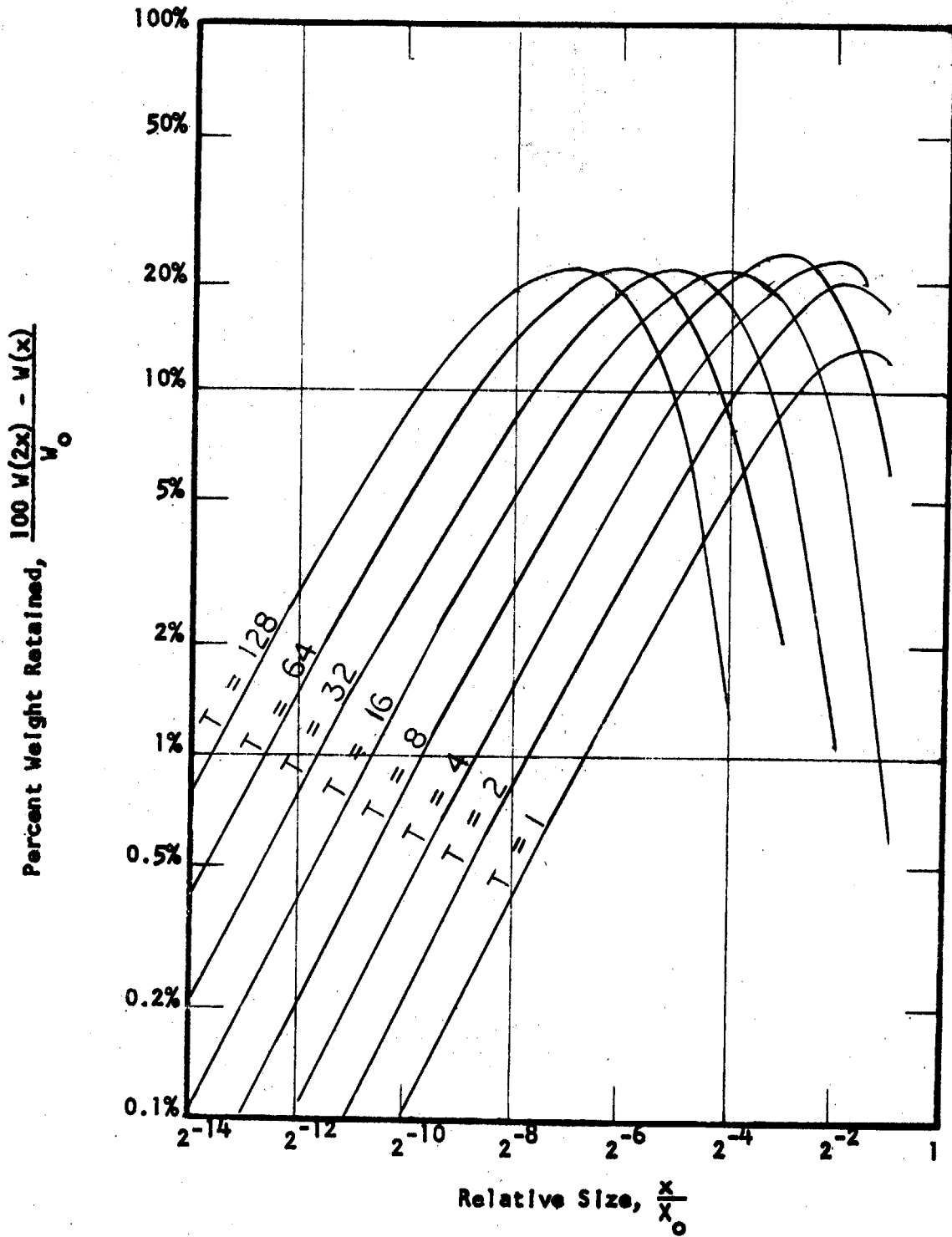


Fig. 18 -- Calculated plots of log percent weight retained vs. log size for different time intervals.  $P(x) = 1/2x$ ;  $r = 4$ .

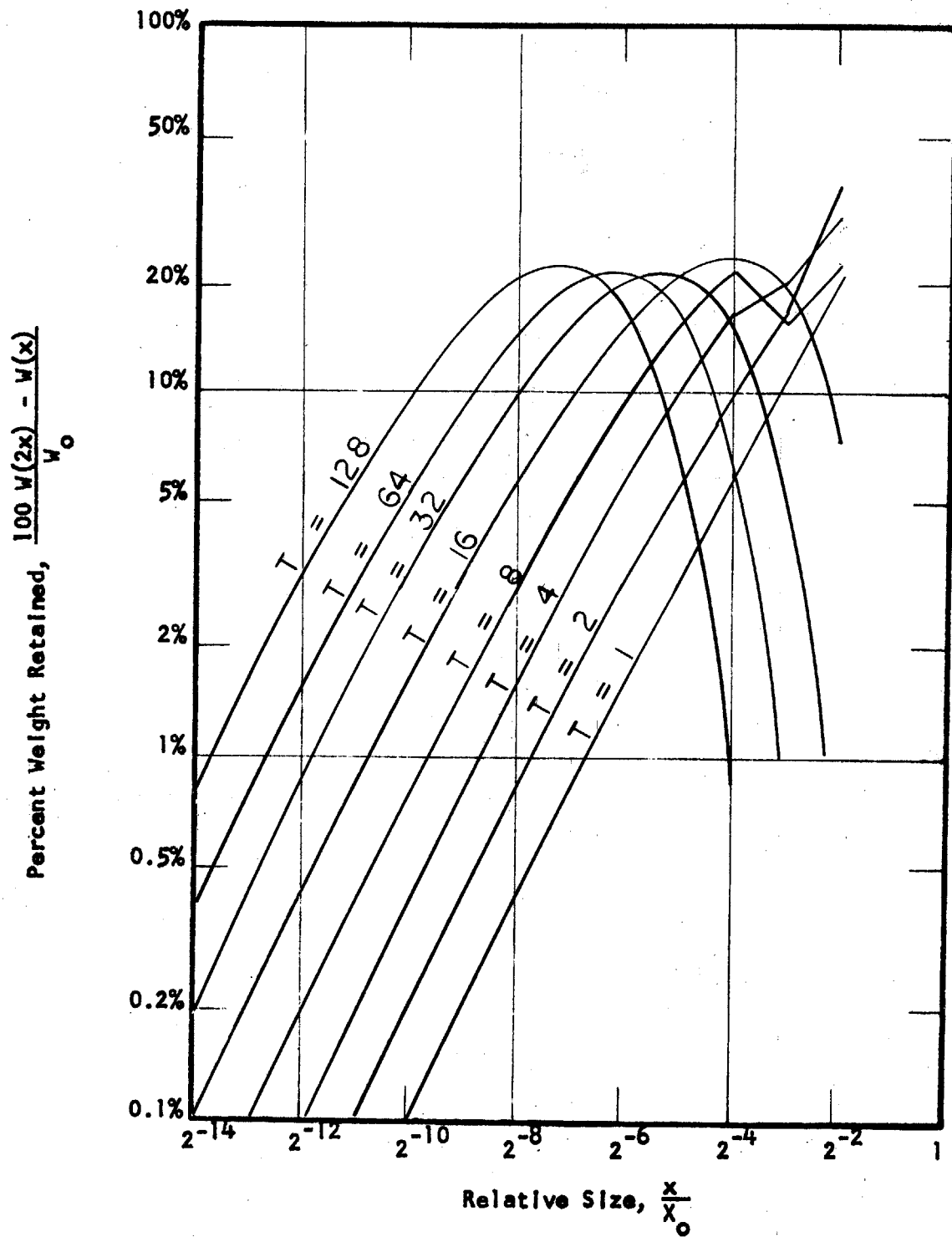


Fig. 19 -- Calculated plots of log percent weight retained vs. log size for different time intervals.  $P(x) = 1/2x$ ;  $r = 4$   $s = 1$ .

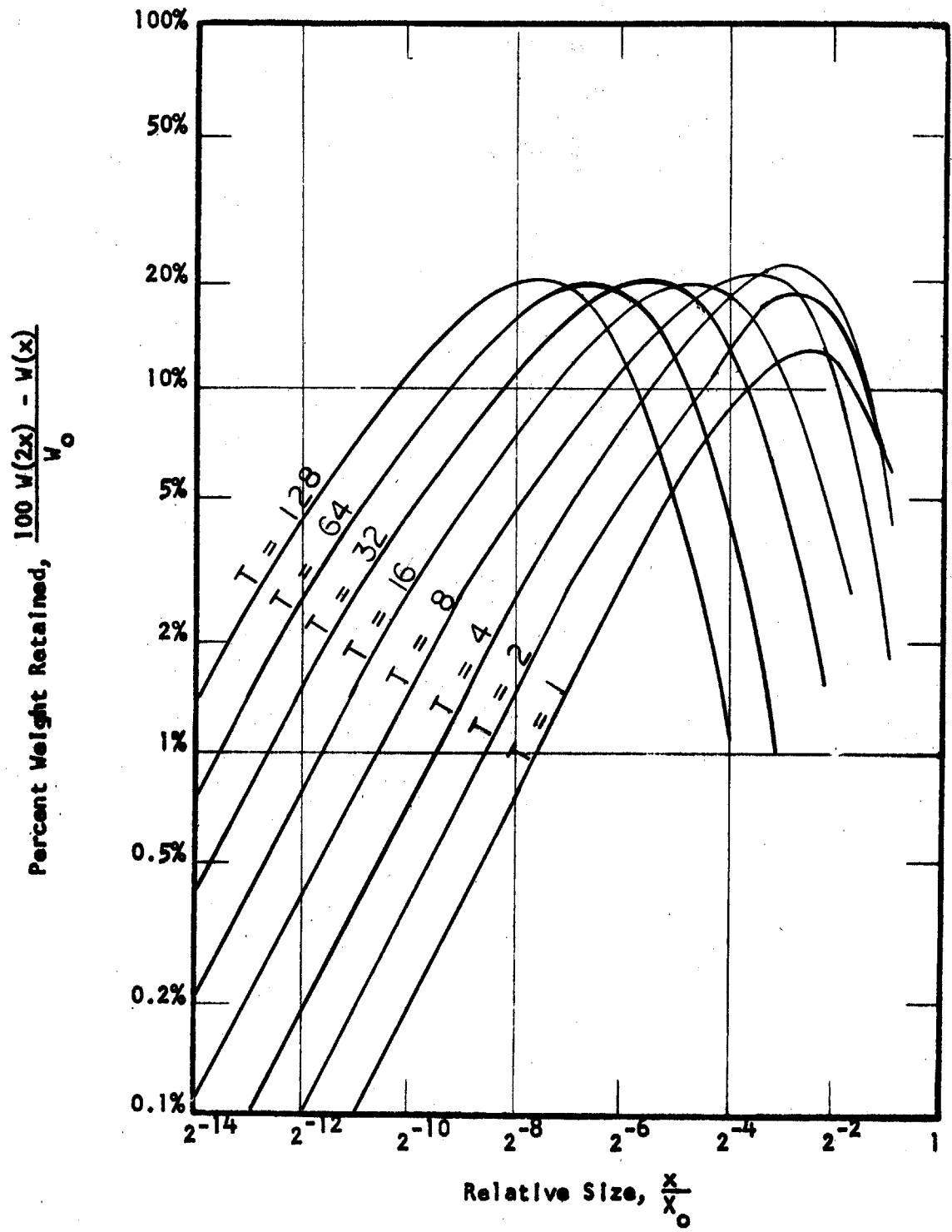


Fig. 20 -- Calculated plots of log percent weight retained vs. log size for different time intervals.  $P(x) = 1/2x$ ;  $r = 8$ .

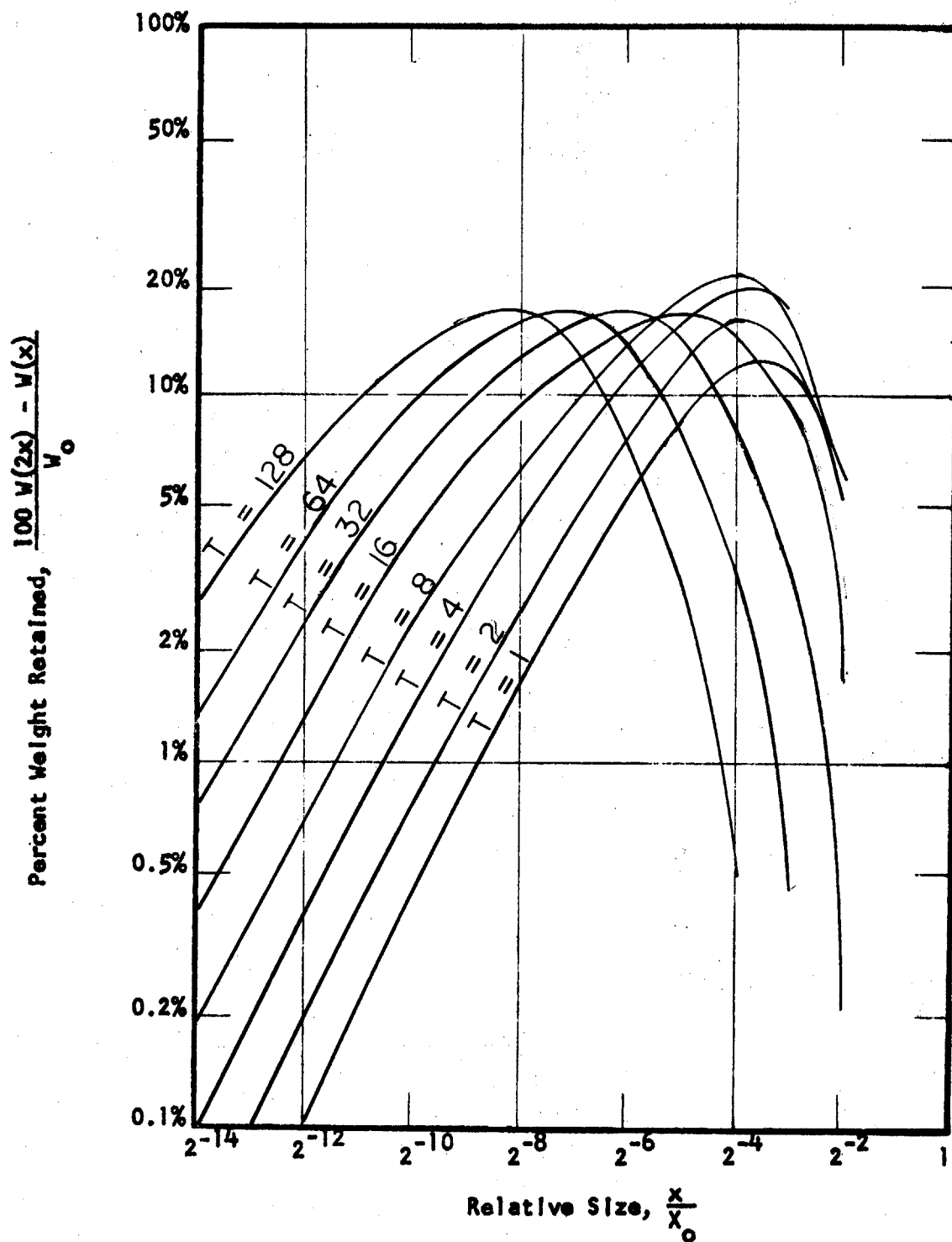


Fig. 21 -- Calculated plots of log percent weight retained vs. log size for different time intervals.  $P(x) = 1/2x$ ;  $r = 16$ .

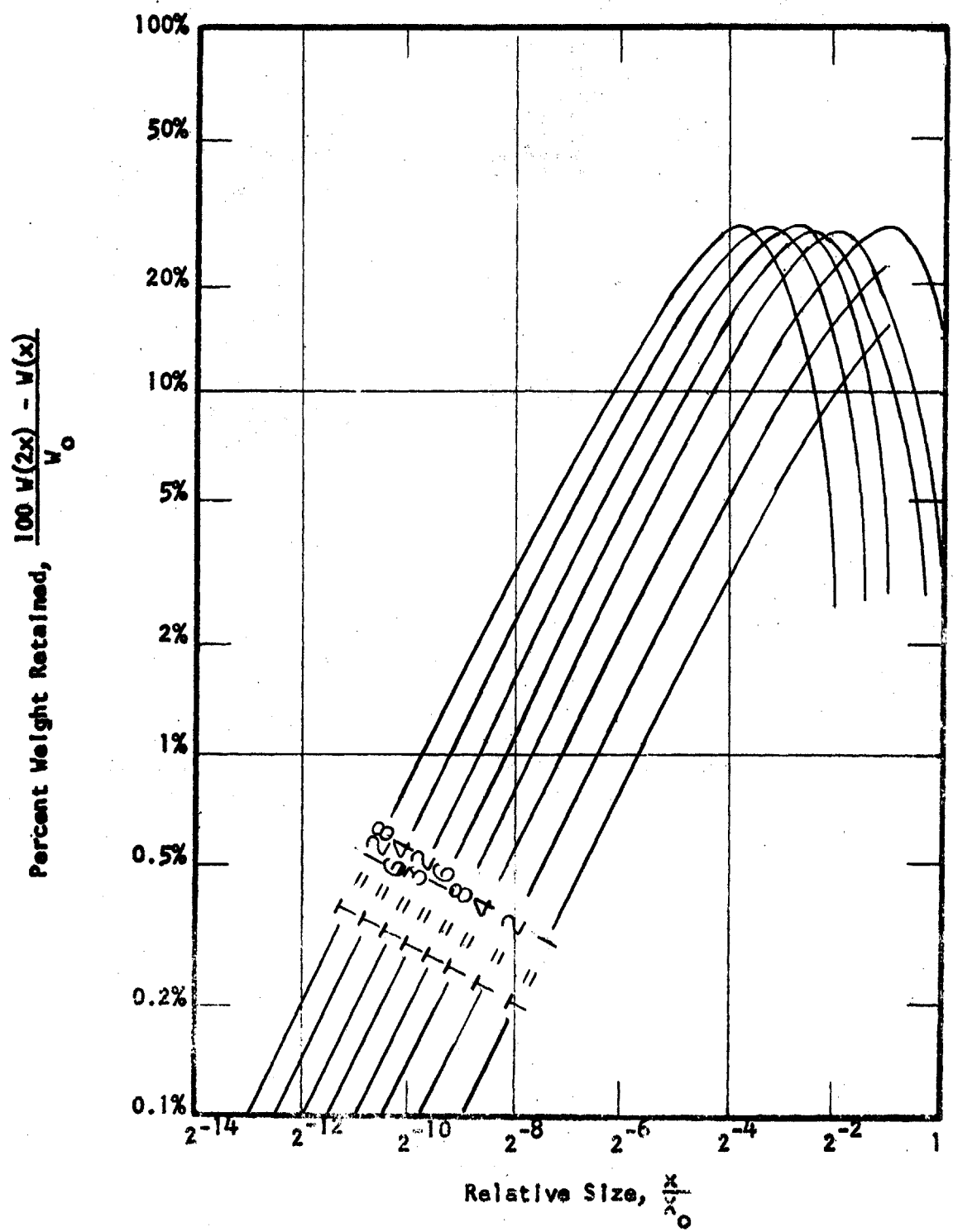


Fig. 22 -- Calculated plots of log percent weight retained vs. log size for different time intervals.  $P(x) = 1/2x^2$ ;  $r = 2$ .



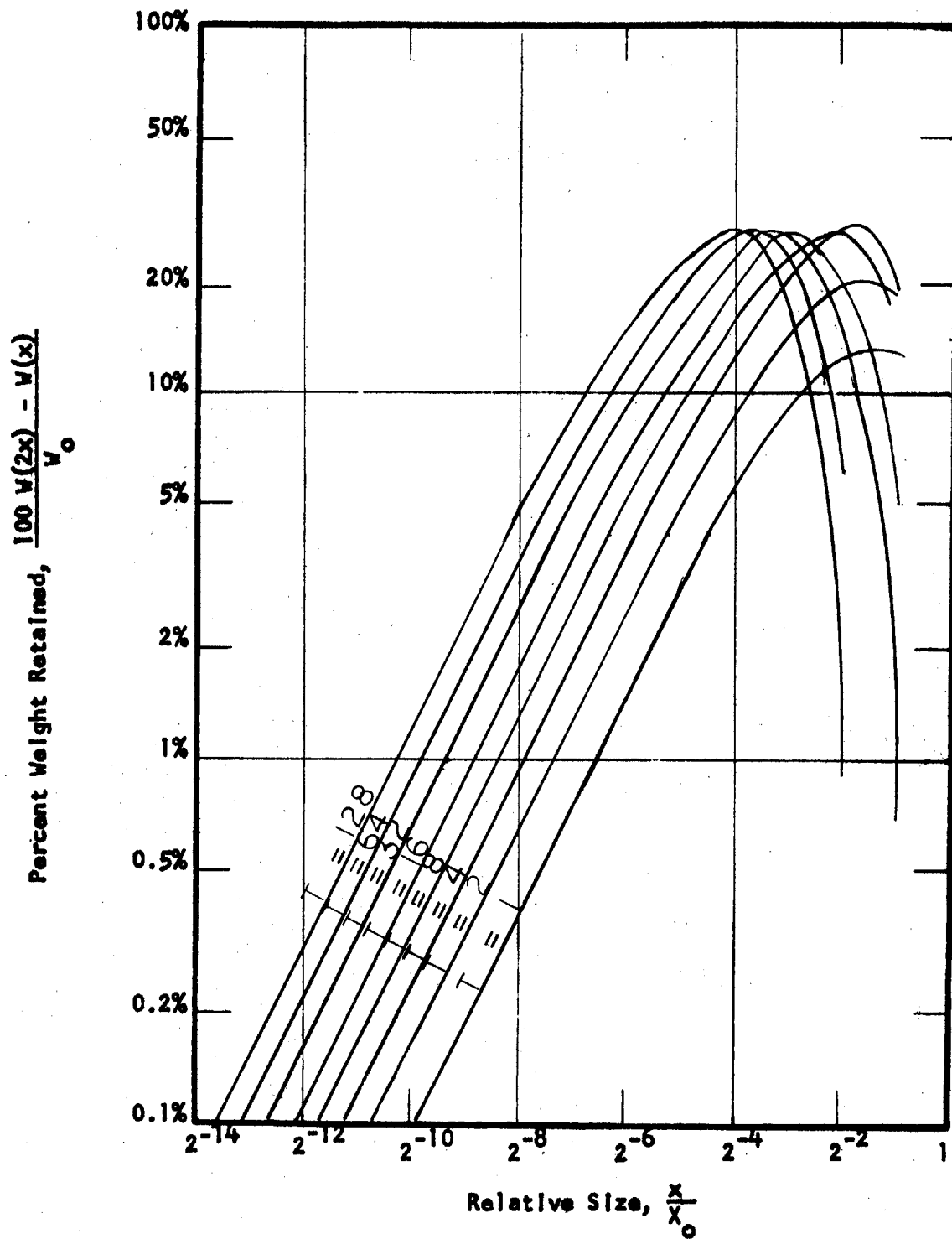


Fig. 23 -- Calculated plots of log percent weight retained vs. log size for different time intervals.  $P(x) = 1/2x^2$ ;  $r = 4$ .

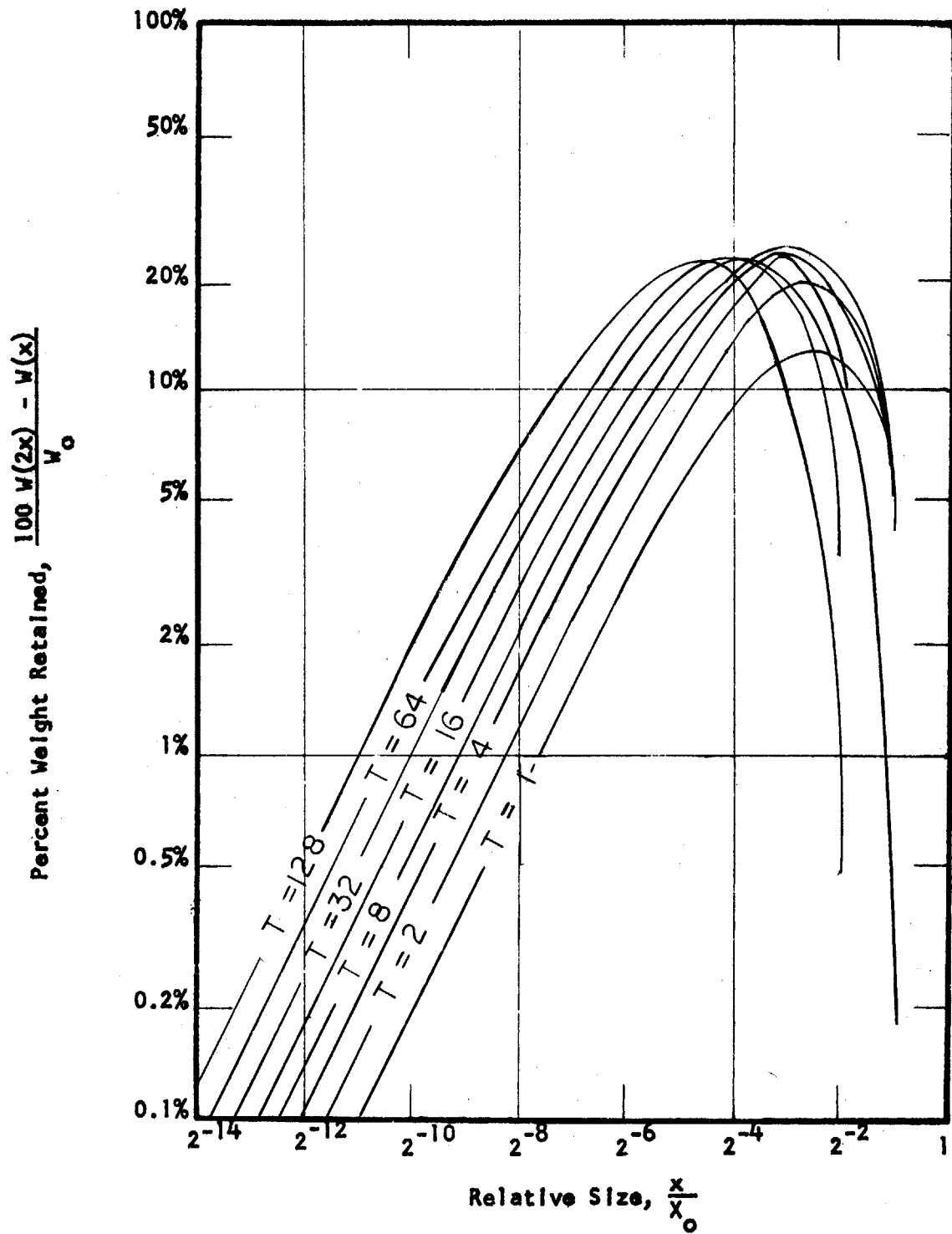


Fig. 24 -- Calculated plots of log percent weight retained vs. log size for different time intervals.  $P(x) = 1/2 x^2$ ;  $r = 8$

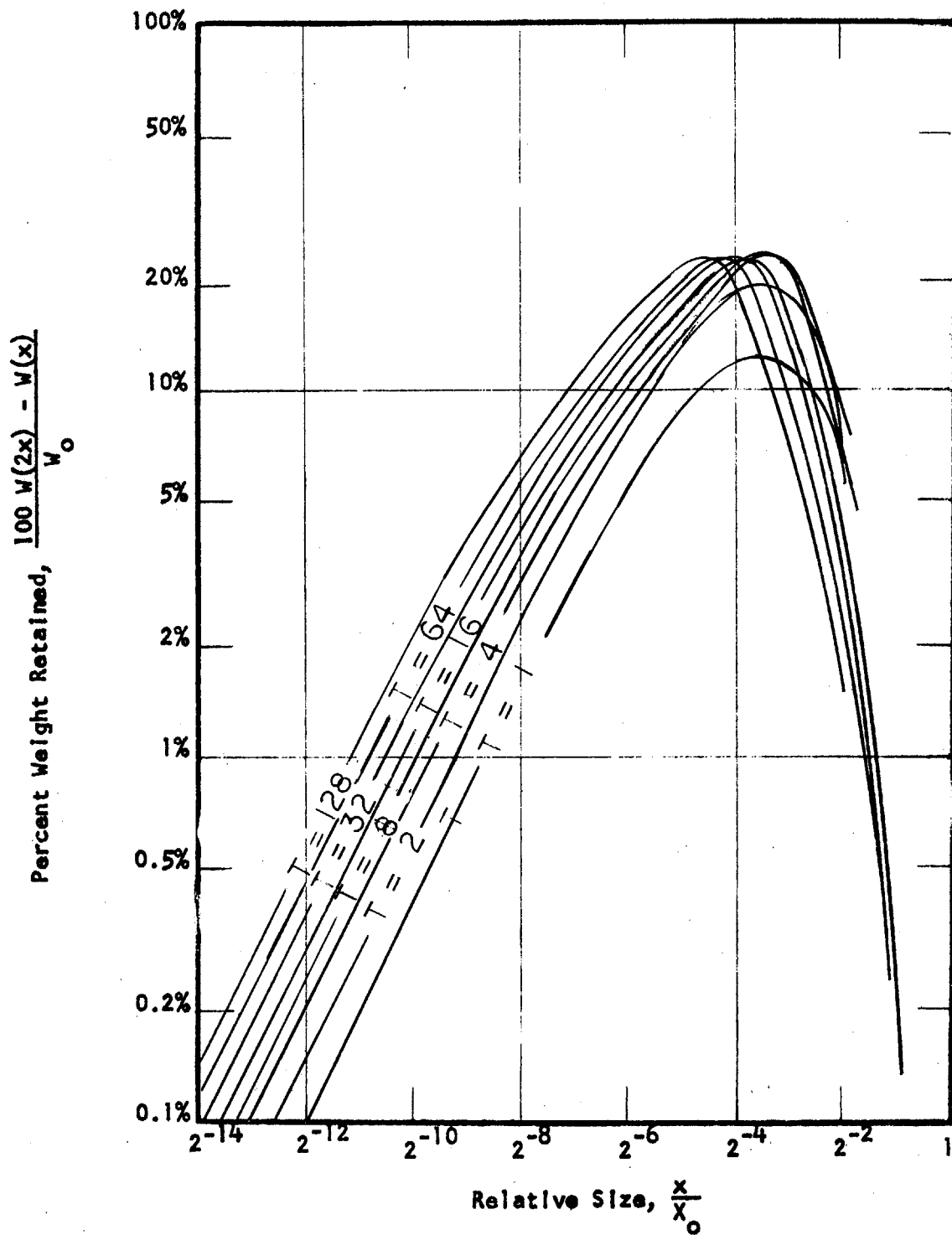


Fig. 25 -- Calculated plots of log percent weight retained vs. log size for different time intervals.  $P(x) = 1/2 x^2$ ;  $r = 16$

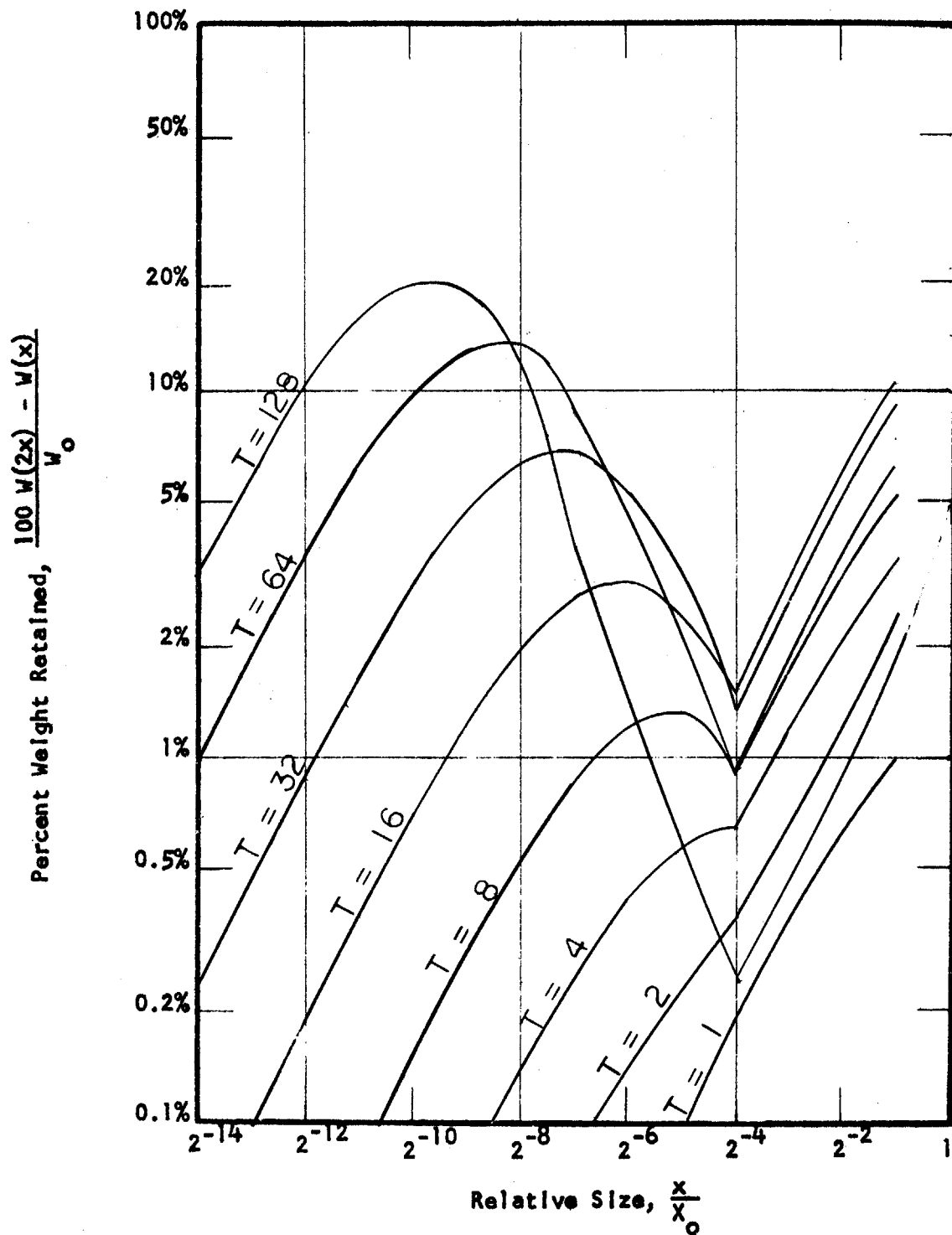


Fig. 26 -- Calculated plots of log percent weight retained vs. log size for different time intervals.  $P(x) = \text{comp 1}$  (See equation 136)  $r = 2$ .

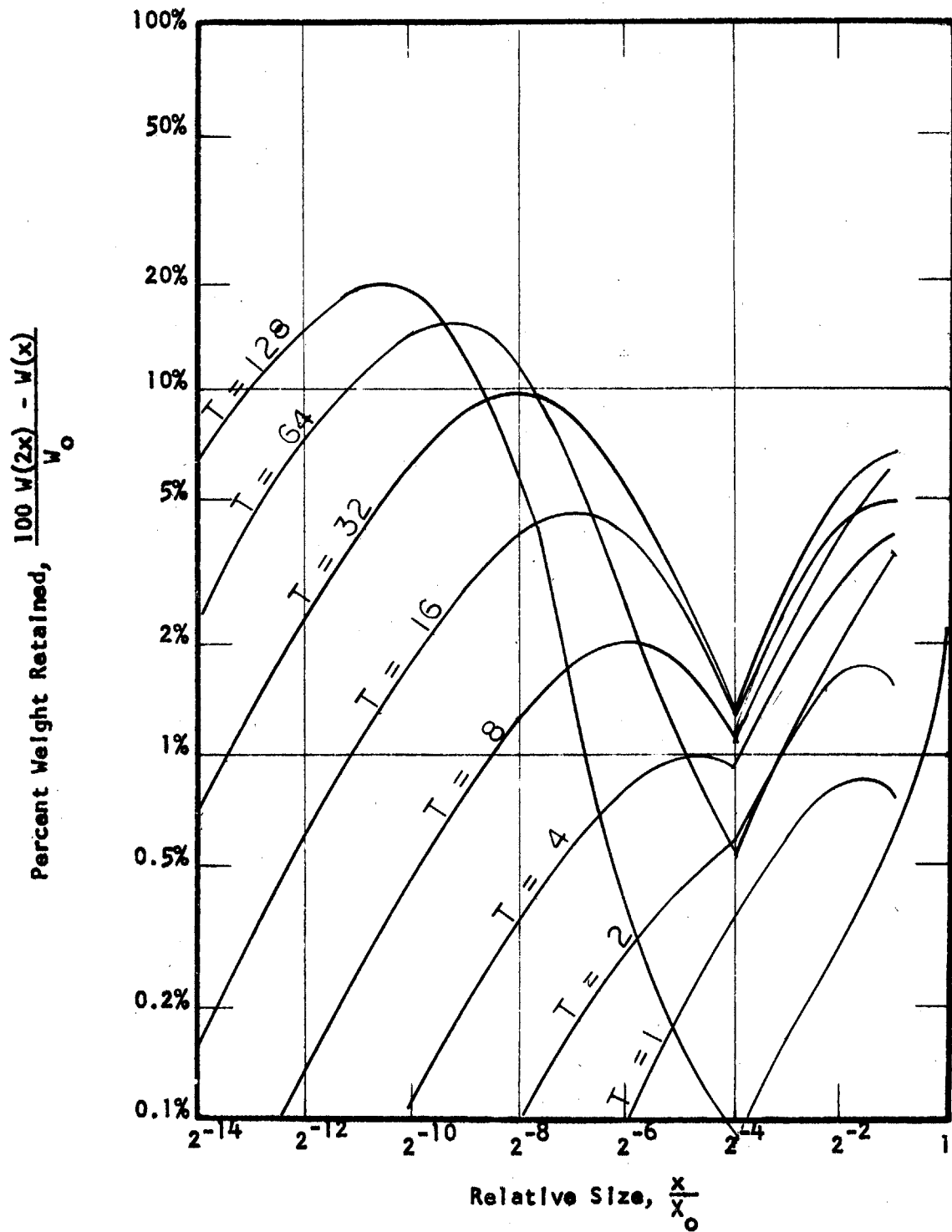


Fig. 27 -- Calculated plots of log percent weight retained vs. log size for different time intervals.  $P(x) = \text{comp 1}$  (See equation 136)  
 $r = 4$

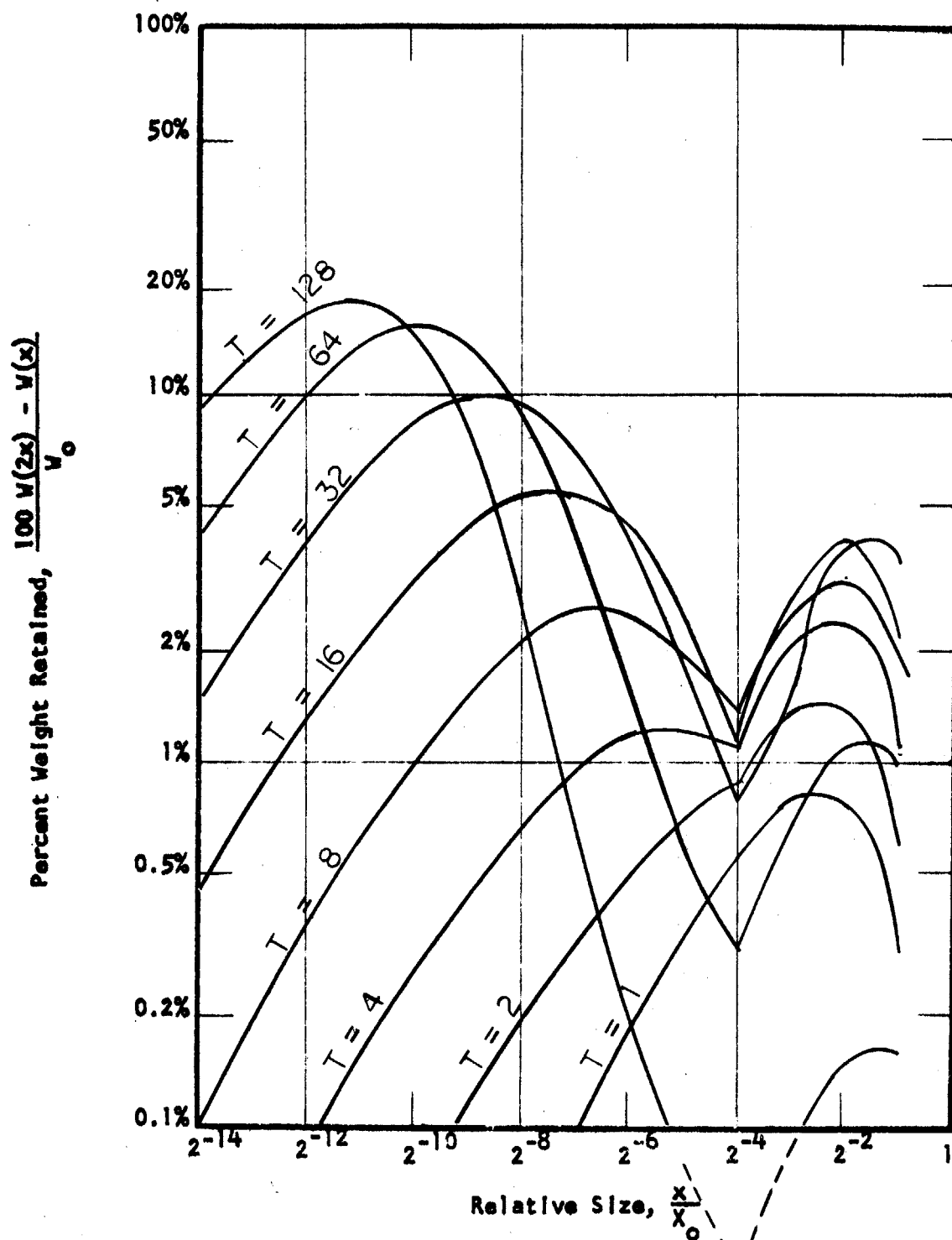


Fig. 28 -- Calculated plots of log percent weight retained vs. log size for different time intervals.  $P(x) = \text{comp 1}$  (See equation 136  $r = 8$ ).

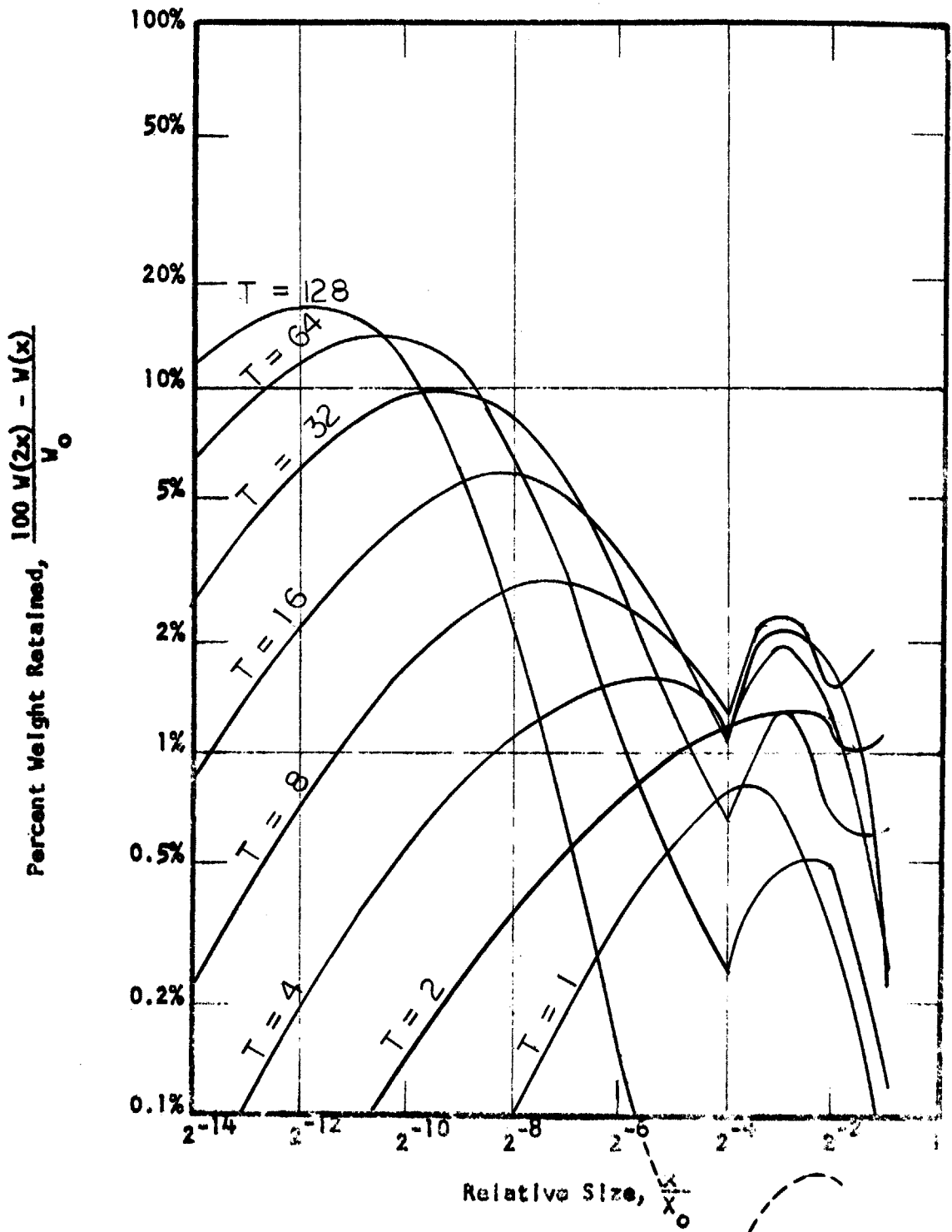
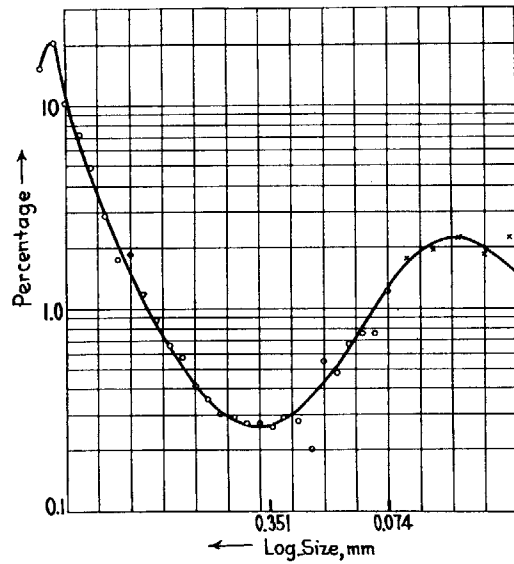
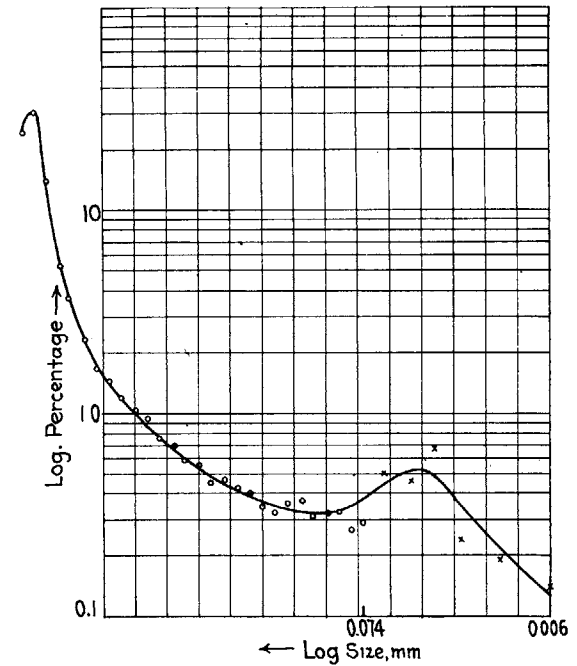


Fig. 29 -- Calculated plots of log percent weight retained vs. log size for different time intervals.  $P(x) = \text{comp 1}$  (See equation 136)  $r = 16$ .



**FIG. 30**—FEED, 2500 GRAMS OF QUARTZ, THROUGH 9.423 MM. AND ON 6.680 MM., GROUND FOR 4 HR. IN BATCH BALL-MILL WITH 55— $\frac{7}{8}$ -IN. BALLS WEIGHING 3500 GRAMS.



**FIG. 31**—FEED, 2500 GRAMS OF QUARTZ, THROUGH 9.423 MM. AND ON 6.680 MM., GROUND FOR 1 HR. IN BATCH BALL-MILL WITH 55— $\frac{7}{8}$ -IN. BALLS WEIGHING 3500 GRAMS.

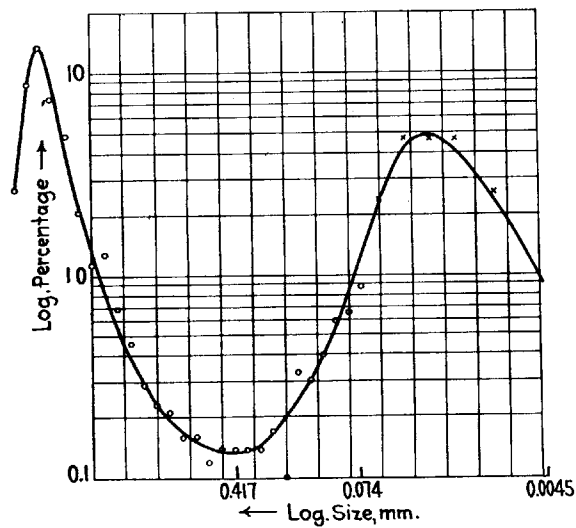


**FIG. 32**—FEED, 2500 GRAMS OF QUARTZ, THROUGH 9.420 MM. AND ON 6.680 MM., GROUND FOR 16 HR. IN BATCH BALL-MILL WITH 55— $\frac{7}{8}$ -IN. BALLS WEIGHING 3500 GRAMS.

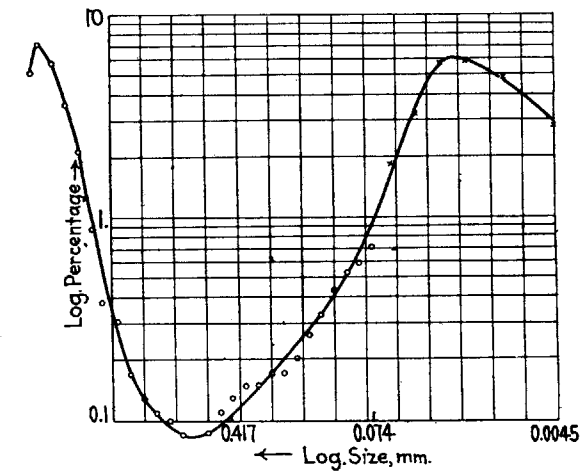


**FIG. 33**—FEED, 2500 GRAMS OF QUARTZ, THROUGH 9.423 MM. AND ON 6.680 MM., GROUND FOR 60 HR. IN BATCH BALL-MILL WITH 55— $\frac{7}{8}$ -IN. BALLS WEIGHING 3500 GRAMS.



## SUMMARY AND CONCLUSIONS

Three major areas of investigation were explored: single fracture, variations of the half-life of a particle with size, and repeated fracture.

The investigation of individual fracture, based on a mathematical model, led to a CWF equation

$$\frac{W(x)}{W_0} = 1 - \left(1 - \frac{x}{X_0}\right)^r \quad (143)$$

As can be seen from figure 2 this equation fits the data well. The mathematical model from which this equation was derived assumed that all fragments of a fracture had the same characteristic shape. This assumption has been verified experimentally insofar as the shape factor has been explored. It is hoped that future work will reveal why particles break this way, for the assumption constant shape implies that the particles are not broken completely at random.

Stamp mills, rod mills and ball mills were the subject of the investigation for determining how the half life of a particle varies with size. From this investigation, a general conclusion was drawn that the probability of a particle of size  $x$  being broken in a given length of time is:

$$P(x) = cx^g \quad (70)$$

where  $c$  and  $g$  are constants. The constant  $c$  depends on the length of time involved, and  $g$  ranges from zero to one or perhaps two. The derived value of  $g$  for a stamp mill is zero; for a rod mill, one-half; and for a ball mill, one. It was assumed during the derivation that all balls or

rods were of the same diameter and that there was no effect of larger particles shielding smaller particles. The simulation of the rod mill was more realistic than the ball mill.

The investigation of repeated fracture led to the development of equation 77, an integral differential equation. When solved, equation 77 expressed CWF as a function of both size and time. The equation was solved analytically for special cases and numerically for a variety of cases. The results of the solution are presented graphically in figures 6-29.

The simulation of the rod mill, figures 11-15, was quite effective. The simulation of the ball mill, figures 16-21 and 26-29 was less effective. This may be due to one of several assumptions made about the ball mill. It was assumed that all particles of the same size broke with the same reduction ratio. This is not likely since some particles of the same size will be more violently broken than others. The second assumption was that the size ratio did not vary with size. Intuitively, this seems false, for smaller particles have less chance to resist the ball than larger particles do. The third assumption was that all balls were of the same size. This is known to be untrue. The fourth assumption was that larger particles do not undergo surface spalling. This is also known not to be the case.

Many of the assumptions that were made were known to be untrue, but were assumed to play a minor role. However, if the model had included these assumptions, it would have been more complicated and would have required far more calculation to determine the effect of the various

parameters. Later work can include the investigation of these parameters.

Figures 26-29 simulate a ball mill where the larger particles have little chance to be broken. These figures resemble those in figures 30-33 taken from Gaudin<sup>(4)</sup>. The direction of increasing size is different for figures 26-29 and figures 30-33. The double hump plus the deep trough indicate that it is relatively easy to simulate this action of a ball mill by assuming that the chance a particle has of being broken increases with size to a maximum and then decreases with size. Once again, only one value of size ratio has been chosen and surface spalling has not been considered.

The ability to simulate the shape of the product of grinding machines by a relatively simple mathematical model is possible. Simple refinements in the model will bring the results closer to that found in practice. In conclusion, this model of comminution is valid for it accurately simulates the output of a comminution device.

## FUTURE WORK

Listed below are some suggestions for future work which are an outgrowth of this dissertation.

1) One of the basic assumptions made in deriving the mass frequency distribution for single fracture of a homogeneous solid was that all fragments have the same characteristic shape. This has been verified experimentally down to size of one micron. However, in the sub-micron range very little is known of the shape of the fragments.

2) The shape of the surface grinding curves in Figure 5 were not simulated by any of the models used. It is suggested that a  $P(x) = \frac{1}{2} x^2$  and a reduction ratio of  $r = 0.1$  might very well simulate spalling in both a rod mill and a ball mill.

3) No effort was made to determine the effect of varying the reduction ratio with particle size. It is suggested that this is probably the case in grinding devices. The writer presumes that the reduction ratio would get smaller with decreasing particle size.

4) No effort was made to use a spectrum of reduction ratios for a given particle size. This certainly is to be expected for not all particles of a given size break in the same manner. The expected effect would be to lower the peak and broaden the base of the curves. The writer would presume that a Poisson distribution of the integers about a chosen mean would be the initial starting point.

5) The model of a ball mill with particles so large that they are unlikely to break worked fairly well. However, other models with other variations in  $P(x)$  should be explored.

6) The problem of grain size and preferential breakage were not considered. It would be a relatively easy matter to set up models of preferential breakage to find out which factors are governing. The models should include variations in the CWF curve for individual fracture, systematic variation of  $r$  so that all sizes would tend to break to a given size, and variations in  $P(x)$  so that larger particles would break easily while smaller ones wouldn't.

7) A major goal is to represent complex materials consisting of two or more phases in a manner whereby the locked particles would be separately tabulated from the free particles of each phase. It is possible to do this now but large matrices are required. Once complex materials can be represented, it is only a short step to analyzing grinding circuits.

8) Once complex ores or materials can be represented, it is a simple step to represent the ore by one matrix, the different machines by another matrix and the feed by another. An actual circuit could be simulated and the product calculated. In fact, one can consider this type of analysis similar to the analysis of an RLC electronic circuit where instead of each element being represented by a pure number, it is represented by a matrix. The resulting calculations would be similar except that matrix algebra would be used.

Using this approach one could set up and analyze the optimum grinding circuit for a given ore.

## BIOGRAPHICAL NOTE

Thomas Phillips Meloy was born in New York City, September 14, 1925. He received an A.B. in Physics from Harvard University in 1949 and a B.S. in Metallurgy from M.I.T. in 1951. From 1951 to 1957 he worked as an engineer for the Air Craft Gas Turbine Division of General Electric Company in Cincinnati, Ohio.

In 1957 he was admitted to the Graduate School of the Massachusetts Institute of Technology. In October of 1960, he presented to the faculty of the Massachusetts Institute of Technology a thesis entitled "Brittle Fracture" in partial fulfillment of the requirements for the Ph.D. degree.

## BIBLIOGRAPHY

1. Minerals Year Book, 1958, Vol. III, Bureau of Mines.
2. R. P. von Rittenger, Lehrbuch der Aufbereitungskunde, (Ernst und Korn, Berlin, 1867).
3. H. Stadler, Grading Analyses and Their Application, Trans. Inst. Mining and Met., 19, 471-485, 509-537 (1910); 20, 420-438 (1911).
4. A. M. Gaudin, An Investigation of Crushing Phenomena, AIME Trans., 1926, Vol. 73, pp 253-316.
5. R. T. Hukki, An Experimental Study of the Principles of Comminution, Sc.D. Thesis, Massachusetts Institute of Technology.
6. R. Schuhmann, Jr., Principles of Comminution, I. Size Distribution and Surface Calculations, AIME T.P. 1189, (1940).
7. J. C. Bennett, R. L. Brown, Broken Coal IV, J. Inst. Fuel, Vol. 14 p. 135 (1941).
8. J. C. Bennett, R. L. Brown and H. G. Crone, Broken Coal II, J. Inst. Fuel, Vol. 14, p. 111 (1941).
9. R. L. Brown, Broken Coal III, J. Inst. Fuel, Vol. 14, p. 129 (1941).
10. P. Rosin, E. Rammler, "Regularities in the Size Distribution of Cement Particles," Zement (1933) Cited by Epstein (11).
11. B. Epstein, Logarithmico-Normal Distribution in Breakage of Solids, Indust. Eng. Chem., Vol. 40 (1948) pp 2289-2291.
12. S. R. Broadbent, T. G. Callcott, A Matrix Analysis of Process Involving Particle Assemblies, Philo. Trans. Roy. Soc. Lon. (1956) Vol. 249 Series A, pp 99-123.

13. S. S. Gilvarry, B. H. Bergstrom, Fracture and Comminution of Brittle Solids, AIME Preprint No. 60B103, Presented Annual Meeting February 1960, N.Y.
14. G. P. Wadsworth and J. G. Bryant, Introduction to Probability Theory and Random Variables, 1960, McGraw-Hill Book Co., New York.
15. Ibid, pages 155-159, Examples 6-8, 6-9, 6-10, and 6-11.
16. A. M. Gaudin, H. R. Spedden and D. F. Kaufman, Progency in Comminution, Min. Eng. Vol. 3, No. 11, (1951) pp 969-970.
17. G. P. Wadsworth and J. G. Bryant, Introduction to Probability Theory and Random Variables, pages 1-2, (1960) McGraw-Hill Book Co., New York.
18. W. Feller, An Introduction to Probability Theory and Its Application Vol. I, Second Edition, 1957, John Wiley & Sons Inc., N.Y.
19. F.B. Hildebrand, Methods of Applied Mathematics, 1952 Prentice-Hall Inc., Englewood Cliffs, N. J.